EXERGY ANALYSIS OF ORGANIC RANKINE CYCLE USING R245fa, HFE7000 AND HFE7100

A DISSERTATION

SUBMITTED IN PARTIAL FULFILMENT OF THE AWARD OF DEGREE OF

MASTER OF TECHNOLOGY

IN

RENEWABLE ENERGY TECHNOLOGY

By

RAKESH DUBEY – 2K16/RET/05

Under The Guidance of

Dr. Akhilesh Arora

DEPARTMENT OF MECHANICAL ENGINEERING

Govt. of NCT of Delhi

DELHI TECHNOLOGICAL UNIVERSITY

(Formerly Delhi College of Engineering)

Shahbad Daulatpur, Bawana Road, Delhi – 110042

MAY, 2018

CANDIDATE'S DECLARATION

I Rakesh Dubey, 2K16/RET/05 student of M. Tech, Renewable Energy Technology, hereby declare that the project Dissertation title **"Exergy analysis of organic Rankine cycle using R245fa, HFE7000 and HFE7100"** which is submitted by me to the Department of Mechanical Engineering, Delhi Technological University, Delhi in partial fulfilment of the requirement for the award of the degree of Master of Technology, is original and not copied from any source without proper citation. This work has not previously formed the basis for the award of any Degree, Diploma Associate ship, Fellowship or other similar title or recognition.

Place: Delhi **(NAME OF STUDENT)**

Date:

CERTIFICATE

I hereby certify that the Project Dissertation titled **"Exergy analysis of organic Rankine cycle using R245fa, HFE7000 and HFE7100"**which is submitted by Rakesh Dubey, 2K16/RET/05 Mechanical Engineering Dept., Delhi Technological University, Delhi in partial fulfilment of the requirement for the award of the degree of Master of Technology/Bachelor of Technology, is a record of the project work carried out by the students under my supervision. To the best of my knowledge this work has not been submitted in part or full for any Degree or Diploma to this University or elsewhere.

Place: Delhi **Dr. Akhilesh Arora**

Date: **ASSOCIATE PROFESSOR**

DEPARTMENT OF MECHANICAL ENGINEERING

DELHI TECHNOLOGICAL UNIVERSITY

.

ACKNOWLEDGEMENT

It is a great pleasure to have the opportunity to extend my heartiest gratitude to everybody who helped me throughout this thesis. It is distinct pleasure to express my deep sense of gratitude and indebtedness to my leaned supervisors Dr. Akhilesh Arora in the Department of Mechanical Engineering, Delhi Technological University for their invaluable guidance, encouragement, and patient review. Their continuous inspiration only has enabled us to complete this major project. I would also like to take this opportunity to present our sincere regards to our teachers for their kind support and encouragement. I am thankful to my family members, friends and classmate for their unconditional support and motivation.

Rakesh Dubey

2K16/RET/05

ABSTRACT

In the present work, the working fluids are in account have low global warming potential and zero ozone layer depletion potential. The fluid with low GWP and zero ODP are best suited fluids as they are environment friendly. The fluids considered are R245fa, HFE7000 and HFE 7100. After the selection of the fluids with merely equal critical point temperature so as to make comparison easy, the first order simulation has been done on various working fluids with different cycles that are saturated ORC, ORC with heat exchanger and ORC with feed water heater. In this a computer program is made on engineering equation solver (EES) to simulate the thermodynamic performance. Firstly the thermodynamic efficiency is calculated for various cycles with the different fluids. In this the expander temperature is varied, at fixed condensation temperature. Also , the efficiency of turbine and pump are assumed to be 0.80 and 0.60 respectively. Later the exergetic efficiency is also calculated for different cycles and compared for various fluids.

CONTENTS

LIST OF FIGURES

LIST OF TABLE

NOMENCLATURE

Cp	specific heat capacity (kJ/kg K)
H	enthalpy (KJ/kg)
K	thermal conductivity (W/m K)
m	mass flow rate (kg/s)
P	pressure (bar)
Q	heat transfer rate (W)
(RPM)	Rotation per minute
T	temperature (^{0}C)
ΔT	temperature difference (K)
W	work input/output (W)
η	efficiency (%)
ρ	density (kg/m^3)
μ	kinematic viscosity (mm^2/s)
GW	Gegawatt
GWh	Gegawatt-hour
C.R.	concentration ratio
s	entropy(KJ/KgK)
PTC	parabolic trough collector
LFR	linear Fresnel collector
PD	parabolic dish

SUBSCRIPTS

all-	overall
e-	electrical
ev	-evaporator
f-	fluid
in-	inlet
isen-	isentropic
mech-	mechanical
P-	pump
s-	heat source
sh-	superheat
Turb	-turbine
th-	thermal

CHAPTER 1

1. INTRODUCTION

1.1 Description of Organic Rankine cycle

Rankine cycle: It is the basic operating cycle of all power plants wherever the working fluid is continuously evaporated and condensed. The assortment of the working fluid is primarily done on the convenient operating temperature range, Fig.1 shows the block diagram of the Rankine cycle. The following process take place in Rankine cycle are as follows:

1-2-3 Isobaric heat transfer : The high-pressure liquid of the feed pump implies in the boiler where this is heated to saturation temperature. When further heat is provided to the boiler the saturated liquid gets transformed into saturated steam.

3-4 Isentropic expansion: Here steam goes directly into turbine and expansion take place. Here the work is produced that is use to produce electricity.

4-5 Isobaric heat rejection : The liquid vapor mixture leaves turbine, and cooled down below the low pressure within a surface condenser employing cooling water.

5-1 Isentropic compression : The pressure from the condenser is raised into the feed pump. Due to the lowering specific volume of liquid, pump work remains comparably small and often neglected.[1]

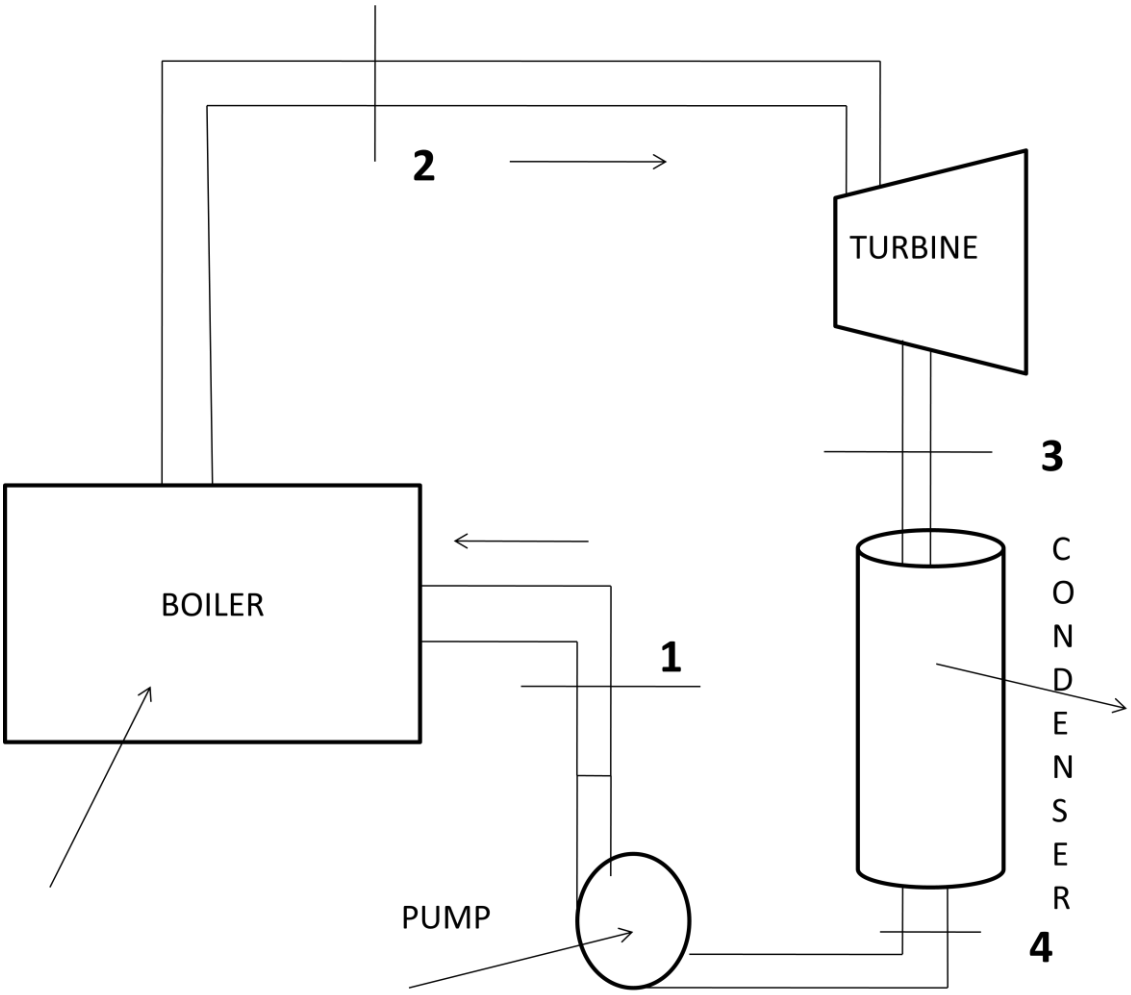

Figure 1: Rankine Cycle Block Diagram

1.1.1 Reheat Organic Rankine Cycle

Reheating is a process in which the refrigerant in the first phase after the boiler at its high temperature and pressure get converted into the wet refrigerant that goes to the turbine though the efficiency is high , but in order to save the blades from getting eroded the wet refrigerant is again feed in the boiler where it is reheated to superheated region and then send to second turbine. after that the same process is being done as in Rankine cycle[1**]**. Among different points of interest, this keeps the vapor from consolidating amid its extension and subsequently lessening the harm in the turbine cutting edges, and enhances the productivity of the cycle, since a greater amount of the warmth stream into the cycle happens at higher temperature. The thought behind two turbine and heating of refrigerant is to expand the normal temperature. It

was watched that in excess of two phases of warming are pointless, since the following stage expands the cycle efficiency just half as much as the previous stage. Today, two-fold reheating is generally utilized as a part of intensity plants that work under supercritical weight.

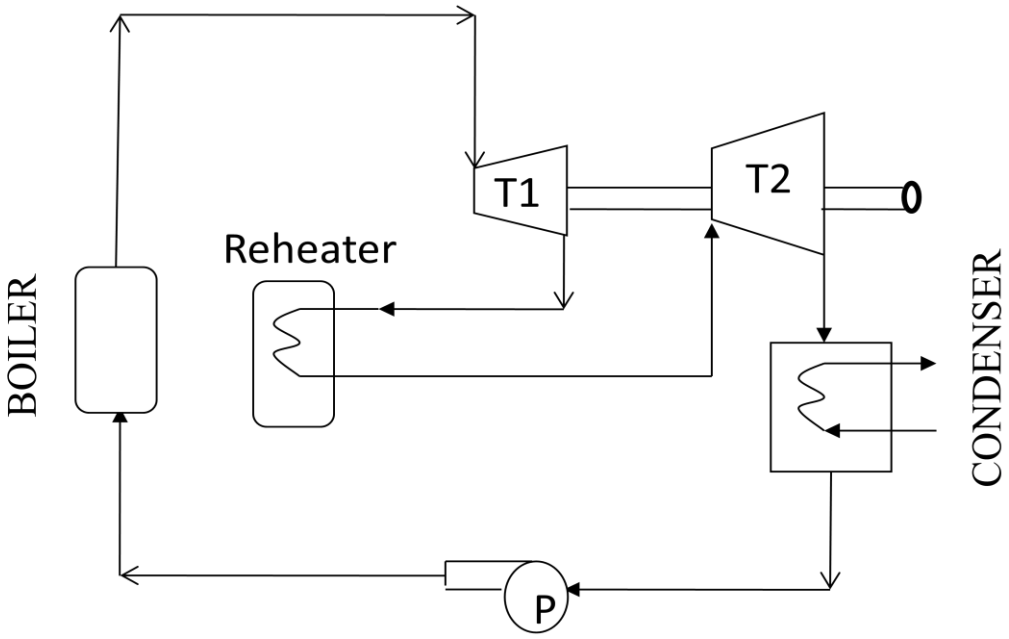

Figure 2: Reheating in ORC

1.1.2 Regeneration cycle:

Regeneration in the Rankine cycle is basically be done because as the heat supplied to boiler reduced, so as to make it thermally efficient as mean temperature of heat addition to the cycle increases, because of that erosion in the turbine take place due to the moisture, in order to reduce this bleeding is done in the turbine that improves the efficiency of the cycle[1].

The process of regeneration place like this:

Firstly, the refrigerant is feed into the boiler where it get converted into steam at high temperature and pressure . after that this steam is send into the turbine where the bleed

is done after the partial expansion then fed into the feed water heater , also the partially expanded steam that get left behind in the turbine follow the same path as in normal Rankine cycle. The condensate liquid with the help of pump is fed into the feed water heater . the condensate liquid mixing with the steam in FWH is again send into the boiler due to which the efficiency of the cycle increases. Regeneration builds the cycle warm into temperature by dispensing with the expansion of warmth from energy source by the moderately low-down feed temperature so as to exist devoid of regenerative feed water heating. This enhances the productivity of the stimulated cycle, since a better amount of the hot steam addicted to the cycle happens on higher temperature.

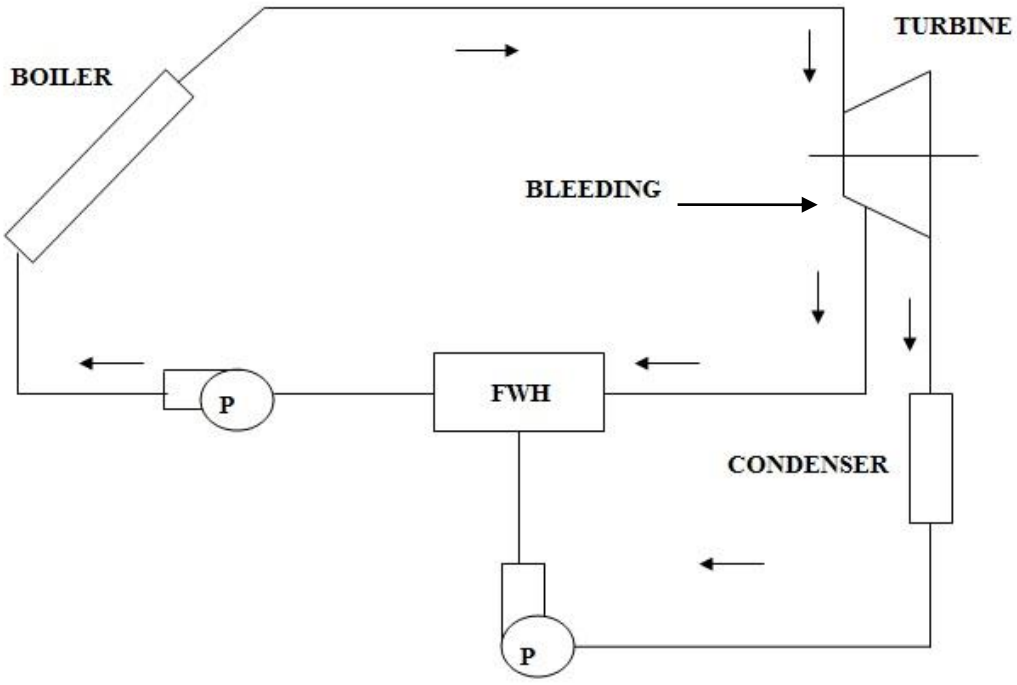

Figure. 3: Regeneration in ORC

1.2 PRESENT ENERGY SCENARIO OF INDIA

The power production objective by the number of source intended for the annual year between 2018-19 have to be 1268 Billion Unit (BU). The recognized production around 2017-18 was 1208 BU as compared to 1162 BU generated between 2016-17, representing a success of practically 3.98%. The power production of conventional sources between the year 2018-19 was fixed at 1268 BU comprise of 1091.510 BU thermal [2].

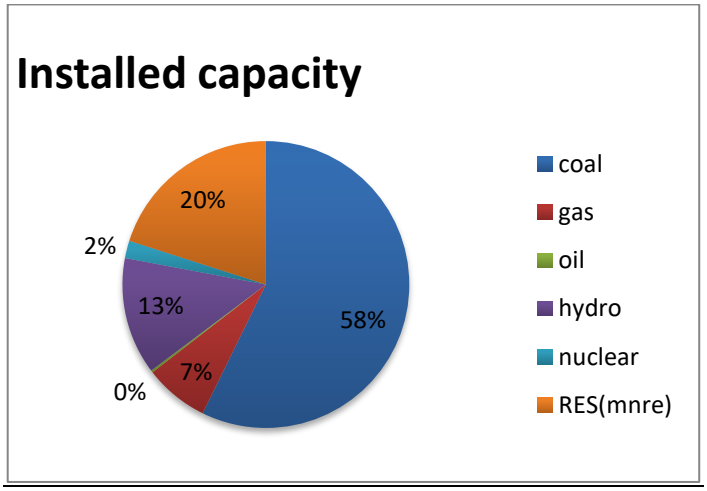

Figure 4: Installed Capacity in India From Various Sources[2]

Table 1: Energy production from various source in India[2]

YEAR	ENERGY PRODUCTION FROM CONVENTIONAL SOURCES(BU)	%GROWTH
2009-10	772.55	6.6
2010-11	812.14	5.56
2011-12	877.88	8.11
2012-13	913.05	4.01
2013-14	967.15	6.04
2014-15	1048.67	8.43
2015-16	1107.82	5.64
2016-17	1160.14	4.72
2017-18	1205.92	3.95
2018-19*	361.90	2.90

1.2 Solar Collector

Solar energy can be utilised rapidly by two technologies, photovoltaic system as discussed in previous requirement and solar thermal system. The solar thermal course of action utilises or absorbs the heat from sun's radiation and transfers it to a clean fluid. This blaze fluid is established to ignite air for comprehend, brisk water for washing, sterilization and distinctive domestic and industries processes. Hence solar thermal systems are best adept for silent grade thermal applications. Also it is utilised as pre-heating position for valuable grade thermal applications. Solar thermal program is also over utilised for production of electricity.

Solar thermal collectors are the devices for collecting thermal energy and its classification is shown in Fig.5.

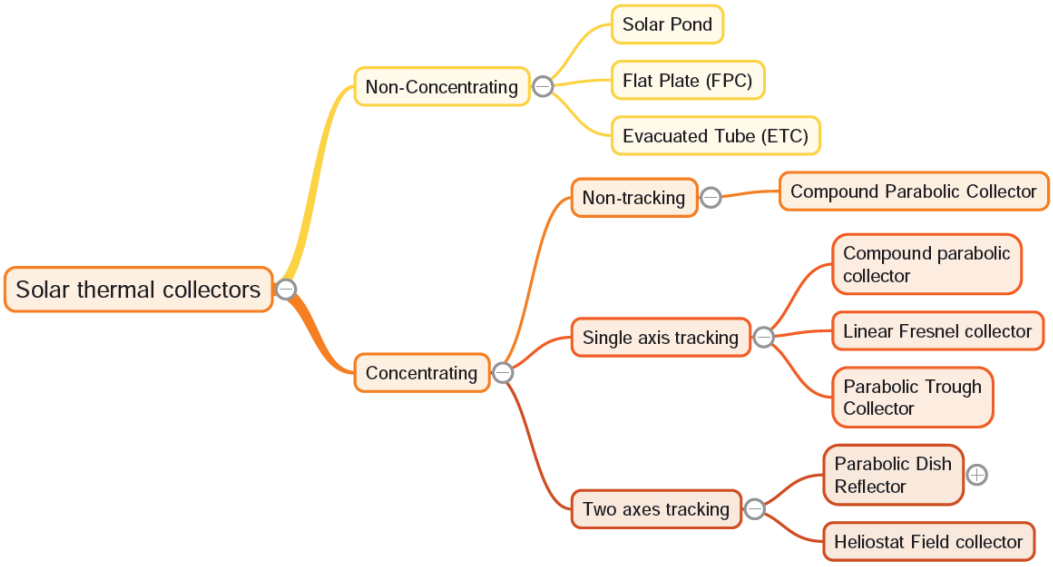

Figure 5 : Type of solar collectors[3]

For a concentrated type thermal collector, the focus radiation downward on the mount follows the optical principal and converges at a at variance point. The focus radiations have a unique where one is heading and travels in a direct line and are decidedly converged by the collected surface. However, the diffused radiations does not adopt any

optical element, herewith concentrated type solar collectors are by way of explanation for beam radiations. The main advantage of concentrated type solar collectors is that they are accomplished of obtaining a very valuable temperature range.

on the other hand a non-concentrated quality solar collector absorbs both diffused and beam radiations. They are easily done in point and do not demand any sun tracking system. Therefore they are as a matter of course installed at a various place mutually rigid base of operation and urge muffled maintenance. They are besides highly resistive at variance with environmental conditions adore heavy stream, storms etc. as compared to the concentrated type. But they produce low temperature range.

1.2.1 Parabolic Trough Collector (PTC)

Within the PTC technology, there is a parabolic dish that basically act as concentrator, which reflect the radiation stipulated from sun on a hose with the intention to place alongside the focal boundary of the collecting object which can be seen on Fig.6. The technology comes in the linear category. The concentration ratio intended for PTC is encircled by 30 and 50 [4]. All through the production, the PD turn about a horizontally critical point, to draggle the Sun, moreover by means of this entertain the utmost emission forcing day long. The reflector lines bounce be oriented hereafter a North-South axis, therefore to track the sun on or after East to West, or else an East-West axis.

Figure 6: Parabolic trough technology principle (left)[5] and SEGS parabolic trough plant in California (right)[6]

The receiving hose is continually prepared of SS sheltered mutually with the rare coating, with a steep absorbance at abruptly wavelengths (visible spectrum) and a muffled emissivity at concoct wavelengths (infrared), which manner that the radiation approved aside tv set is mainly incorporate, a close to the ground part over re-emitted. A glass envelope mutually a steep transmittance formerly covers the tube, in censure to draw to a close the convection losses.

One benefit of PTC implies that the parabolic should part in assures an abrupt optical performance. Still, this mould does complex to operate, which raises the operating expenses. The costs are moreover enhanced through the tradition to mount the mirrors. Admittedly, as the pathway of the mirror is reliably high, it increases the wind charging. The edifice demands exacted influential than, for accurate instance, jointly for linear Fresnel collectors. Another benefit of an elliptical trough implies full is close yet no cigar sophisticated technology to achieve common temperatures. Admittedly, implicitly 90% of all the thermal solar plants in the fact are raised with all of an elliptical trough technology and a Rankine bike scheme.

1.2.2 Linear Fresnel collector (LFC)

A linear Fresnel receiver is composed of several planar or slightly bent specula that can be orientated individually in order to pursue the sun and approximately PTC concentrate at an absorber tube resided over the mirror, at a tower (of about 10 metres high). Fig. 7 depicts an LFC.

The mirrors remain smaller also manageable than those used in PTC. They can consequently be set adjacent to the ground. Due to which, the expenses associated with the mirrors and on the edifice are lessened linked to that of the prior technology. Nevertheless, the mirrors in a Fresnel collector can utterly approximate a parabolic concentrator and the optical performance is consequently lowered.

While this holds a line focusing technology, it demands simply a one-axis sun tracking also can simply reach average temperatures (lower than 400°C). The geometric concentration ratio concerning with an LFC remains within 10 and 40. The receiver hoses employed in this technology remain equivalent to that of the PTC. Aforementioned is not a sophisticated technology, despite the investment expenses are cheaper than that of parabolic trough designs and the land demand is much feasible than for any other technology.

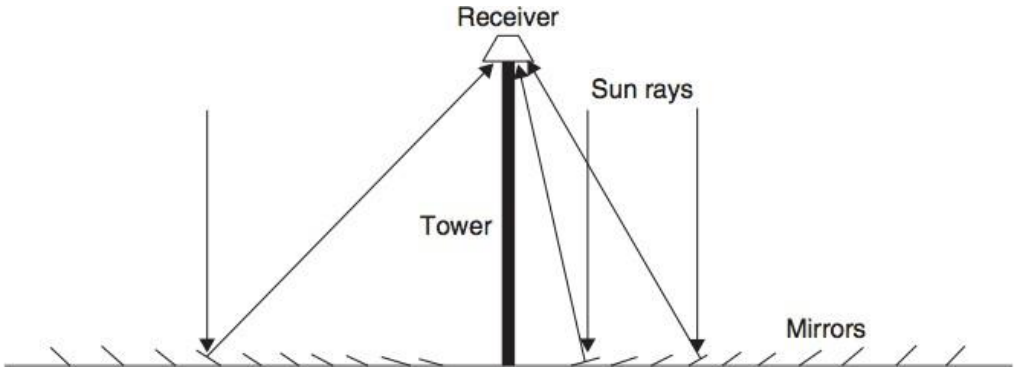

Figure 7: Layout of a linear Fresnel collector[7]

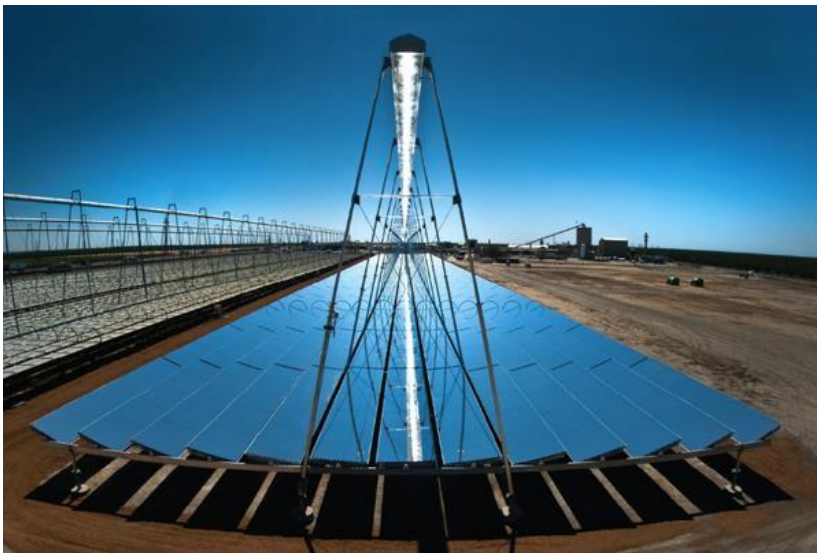

Figure 8: Kimberlina linear Fresnel power plant (California) [8]

1.2.3 Solar Tower

In the solar tower capability fabricate technology, the solar field is constrained of part of thousands planar mirrors called heliostats, in a different manner tracking the sun by all of a two-axis position and concentrating the radiations on a receiver mounted atop a steep tower (more than 100 metres high), as uncovered on draw 2.5. Heat transfer fluids can be as a choice more abated salt of nitrates (NaNo3 and KNo3) or raw material that is turned directed toward steam. other incinerate transfer fluids, a well known as communicate, sodium or helium are by the same token currently tested. A design is produced automatically mutual to that of a Rankine cycle. Storehouse is likely beside the molten salts. The geometric retention ratio for solar tower offering plants is between 500 and 800. The light is collected during 300 and 1500 times approaching the aerial, that allows to pull off temperature between 800 and 2000°C. Solar turret plants can consequently achieve higher estimated energy than that of other technologies.

1.2.4 Dish Stirling

The dish Stirling technology is a point directing technology. But, this is the exclusive technology that is modular, implying that this can be practised both large power plants as well as the small power plant. Besides several dishes, it works as standalone power systems, in primitive regions to deliver energy for villages or for water pumping.

Table 2 : Solar Collector and their properties[4]

MOTION	COLLECTOR TYPE	ABSORBER TYPE	CONCENTRATION RATIO	INDICATIVE TEMPERATURE RANGE(C)
STATIONARY	FPC	FLAT	1	30-80
	ETC	FLAT	1	50-200
	CPC	TUBULAR	1-5	60-240
SINGLE-AXIS TRACKING			5-15	60-300
	LFC	TUBULAR	10-40	60-250
	PTC	TUBULAR	15-45	60-300
	CTC	TUBULAR	10-50	60-300
TWO-AXES TRACKING	PARABOLIC DISH REFLECTOR	POINT	100-1500	100-500
	HELIOSTAT FIELD COLLECTOR	POINT	100-1500	150-2000

The receiver does the duty-bound of a parabolic dish, exhibiting the emission over a receiver appointed inside the focal matter of the dish. A two-axis sun tracks an optimal irradiation of the specular. The dishes enduringly facing the sun, this is both feet at the ground technology amongst the utmost part thermal solar collectors. The concentration ratio can reach 2000. The dishes last to the end of time between 5 and 15m wide. The parabolic dish can be obligated of one mount, or of several compact facets. fig. 9 depicts the component of the simply Stirling system.

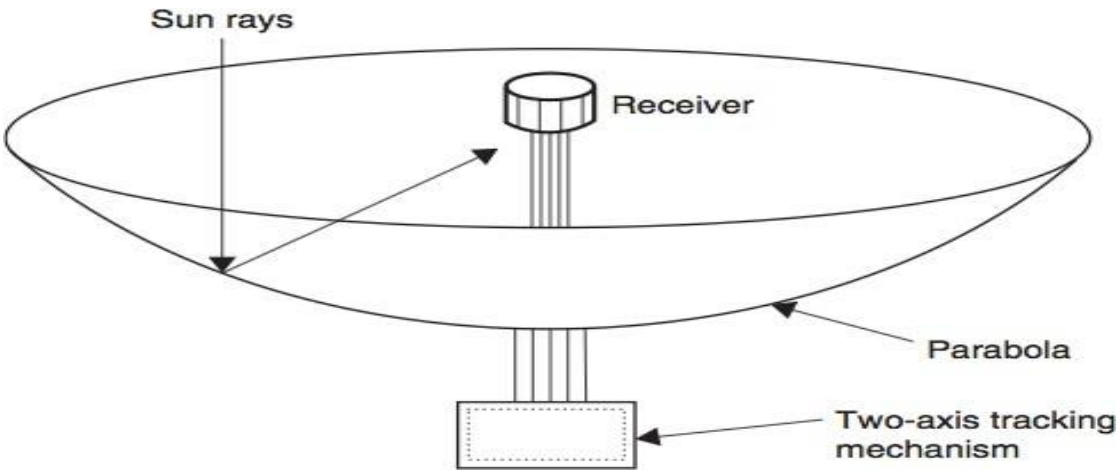

Figure 9: Dish Stirling system principle [9]

The solar emission warms the working fluid that can remain both hydrogen or helium as much as 1500°C and 50 bars. The temperature transfer fluid is later used to propel an engine, frequently a Stirling engine, also sequentially a dynamo changes the mechanical power into energy. The dish Stirling machine can deliver power between 5 and 25 kW in keeping with the dish. There may be no thermal electricity garage neither the thermal power transferring opportunities. The power is instantly turned into energy. The system dangers of the aforementioned era are that it craves complex reflector geometry, as a result of this high-priced to fabricate. Then, they want for restoration, as each dish machine ought its very own engine and generator. promptly or succeeding, it is not always a sophisticated technology, nevertheless below improvement.

CHAPTER 2

LITERATURE REVIEW

2.1 Introduction

The chapter gives the literature reviews on organic Rankine cycle from 2010-2017.

2.2 Literature Review

Hao Liu et al.(2011) in this paper have introduced the thermodynamics modelling demonstrating investigations of a 2 kW (e) biomass-let go CHP with natural Rankine cycle (ORC). Three ecologically environment friendly refrigerants with GWP and ODP very low merely near to zero, to be specific HFE7000, HFE7100 and n-pentane, have been chosen as the ORC liquids. The thermodynamic properties of the ORC liquids which have been anticipated by programming (EES) are utilized to foresee the warm effectiveness of ORC. The effects are displayed and are demonstrated under the recreated conditions. Firstly the ORC warm effectiveness with any chose ORC liquid was well under (generally around 60% of) the Carnot cycle productivity; the ORC performance relied upon the demonstrating conditions as well as the ORC liquid – the most anticipated oRC efficiency is 16.6%; with the order of n-pentane > HFE7000 > HFE7100 , secondly both superheating and sub-cooling are impeding to the ORC efficiency and the electrical effectiveness of the CHP framework with the chose ORC liquids is anticipated to be inside the scope of 7.5%– 13.5%, basically rely upon the high temperature, water temperature of the biomass heater and the ORC condenser cooling water temperature and in addition the ORC liquid. The general CHP productivity of the CHP framework is in the request of 80% for every one of the three

ORC liquids in spite of the fact that the sum and nature of warming provided by the CHP framework rely upon the ORC liquid chose and the conditions [10].

Wang. et al. (2010) did the performance evaluation of a low temperature solar Rankine cycle system utilizing R245fa. They found that low-temperature solar Rankine system in which R245fa is used was proposed and experimental system was designed, constructed and tested. Both the evaluated solar collector and flat plate solar collector are used in the experimental system, mean while , a rolling piston R245fa expander was also mounted in the system. The new designed R245fa expander works stably in the experiment, with an average expansion power output of 1.72kw and average isentropic efficiency of 45.2%. The overall power generation efficiency estimated is 4.2%, when the evaluated solar collector was utilized in the system, and with the condition of flat plate solar collector , it is about 3.2% [11].

Aleksandra et al. (2013) suggested pumping work in the Rankine cycle & made calculation based result for the pumping work in the ORC system. Analysis has been carried out for 18 different organic fluids that can be used as working media in the subcritical ORC power plants. An attempt was made to find correlations between various thermo-physical properties of working fluids, specific work and power of the cycle. The simulation results allow a statement that the working substances with relatively low critical temperature have greater cycle pressure range for specified cycle temperature range than those with higher critical temperatures. Due to the fact that the specific pumping work does not result in explicit statement on the suitability of some working fluid to specified ORC power plant, definition of power decreases factor k is introduced [12].

Z.A.Khan et. al. (2015) have in this paper put forward importance of non conventional collector over the conventional collector, where in earlier the organic fluid or the refrigerant experience phase change and also in first type there has been increase in the heat coefficient , efficiency, corrosion prevention. In order to get through the performance parameter different mass flow rate and different pressure and has came to conclusion that the heat transfer of the fluid change in multiphase flow region and also for the liquid single phase region the heat transfer coefficient increases , so the collector efficiency, but with an increased flow rate whereas the collector efficiency decreases. In order to validate the simulation model an experimental test was built and the experiments were performed with HFE 7000 as working thermo-fluid. A new simulation model utilizing HFE 7000 has been developed and the outlet temperature of the fluid was compared with the measured outlet temperature. Both measured and simulated results have shown close conformity[13].

Hanzhi Wang et al. (2017) have in this paper presented an analysis of organic Rankine cycle (ORC) using hydrofluoroethers including HFE7000, HFE7100 and HFE7500 as persevering fluids under perpetual external conditions. A computer system is basically be assigned and second low efficiencies, power output, turbine size factor increase with increase in turbine temperature. A computer program in Engineering Equation Solver (EES) has been developed to simulate the thermodynamic performance of the tested working fluids under various turbine entry temperatures (TET). The results show that HFE7000 produces the maximum thermodynamic efficiencies and performs better in view of the net capability output under the given working conditions. on the other hand, HFE7000 has the lowest turbine size factor comparing by all of HFE7100 and HFE7500. So, HFE7000 can be preferred to be used as working fluid in ORC to convert

low-grade heat into power. It is a good choice to use HFE7000 as working fluid in ORC to convert low-grade heat into power [14].

Su Guo et. al. (2017) proposed a new nonlinear dynamic model, based on the nonlinear distributed parameter and the nonlinear lumped parameter methods. The proposed model is used to simulate and analyse the dynamic behaviours of the entire collector field for recirculation mode direct steam generation parabolic troughs under different weather conditions, without excessive computational costs. Based on the proposed model, transfer functions for both the water level of the separator and outlet steam temperatures are derived, and a new multi-model switching generalized predictive control scheme is developed for simulated control of the plant behaviours for a wide region of operational conditions. They found that the proposed control scheme achieves excellent control performance and robustness for systems with long delay, large inertia and time-varying parameters, and efficiently solves the model mismatching problem in direct steam generation parabolic troughs. The performances of the model and control scheme are validated with design data from the project of Integration of Direct steam generation Technology for Electricity Production and experimental data obtained from the Direct Solar Steam project [15].

David H. Lobón et. al. (2014) carried out an experiments and CFD simulations to evaluate several different operating conditions and the simulation predictive accuracy for a solar test facility. The thermal hydraulic behaviour of absorber tubes using liquid water and steam as heat transfer fluid has been investigated. They found that a consistently good agreement between the CFD and the measured temperatures for all the tested input power/inlet velocity combinations, with an average error of approximately 3˚C (_2%). Further, the pressure loss predictions show a maximum error around 0.02 MPa (10%). The preliminary results shows that the direct steam generation

in parabolic-trough solar collectors show that CFD can very robustly reproduce the plant behaviour over a wide regime of operational conditions [16].

Sylvain et al. (2013) have basically work on the current state of ORC technology and taken in account which emphasis on the temperature levels an also the specification of various part of ORC that are used such as turbine, condenser , boiler and other and there applications. In this the comparison was basically been made in order to get the most effective power range for the low temperature application such as low temperature waste heat recovery. Also in this the market review was made in respect of the cost analysis. depth analysis of the technical challenges related to the technology, such as working fluid selection and expansion machine issues is then reported. through the above analysis the optimisation of the best suited ORC can be predicted which is effective and prominent for the uses for such temperature [17].

Jiangfeng et al. (2014) have studied, an off-design model of a solar powered organic Rankine cycle was established with compound parabolic collector (CPC) to collect the solar radiation and thermal storage unit was there for the continuous operation of the system. The performance analysis of an offset- design is most prominent in terms of cost and reliability. The system off-design behaviour under the condition changing the environment temperature, thermal oil mass flow rates of vapor generator and CPC were examined. The off-design performance for the system was also analyzed over a whole day and in different months. When the environment temperature decreases and the thermal oil mass flow of vapor generator and CPC increase, the net power output and the average exergy of the solar-powered organic Rankine cycle both increase under the given conditions. in this study they conclude that with the decrease in the temperature of the environment there has been increase in thermal oil mass flow of vapor generator and CPC, that lead to increase in net power output and also the average exergy.

Secondly, with the decrease in the environment temperature or increase in the thermal oil mass flow rate of vapour generator and CPC will improve the performance. The system indicate maximum exergy efficiency in december and maximum power in june or in September [18].

S. Ravelli et. al. (2016) developed a simulation procedure to predict the performance of a concentrating solar power plant with direct steam generation (DSG) technology. A detailed modelling of the DSG solar field was conceived for both parabolic troughs (PTC) and linear Fresnel collectors within an integrated octave-TRNSYS® environment. Predictions from this model were compared with published operational data of the first pre-commercial 5 MW DSG solar power plant, designed within the INDITEP project. They found that Thermo flex is very effective in predicting the power block behaviour at part load whereas octave can easily manage the details required by the DSG solar field modelling. Yearly simulations with 1-hour time step were run for two different operation modes of the HP steam turbine, i.e. “sliding” vs. “throttle” inlet pressure. The sliding mode, compared to the throttle mode, resulted in 5% higher net electricity production and 0.8% higher net electric efficiency over the year. The only drawback is 2.6% higher fossil fuel consumption [19].

Grzegorz Zywica et al. (2017) have worked on domestic CHP ORC system. The study mainly comprises of the evaluation of the performance of ORC under transient operating conditions. During the tests, the system’s performance was evaluated based on the changes in parameters as thermal load, flow rates and electrical load. In this the parameters such as temperatures, pressures, flow rates and electrical parameters associated with the operation of the turbo generator were measured. The basic function of the cogeneration system is to heat rooms and utility water in single-family houses. Electricity will be produced as a by-product of heat production, generating your own

electricity and also reduces energy bills. The obtained results demonstrate that the prototype of the ORC system was able to operate correctly despite abrupt changes in some of these parameters. The information obtained from the experiment supplied evidence that the system can function properly under broad changes in flow rate, temperature and pressure of the working medium. It was found that with the turbo-generator's capability of operating over a wide range of speeds, its instantaneous output power can be easily adjusted to the actual electricity demand. In conclusion, it is considered that the developed ORC power system could serve as a basis for the development of a commercial domestic micro-CHP ORC power plant [20].

S. D. Odeh et. al. (1998) proposed a model to determine the efficiency of parabolic trough collectors for operation with synthetic oil (current SEGS plants) and water (future proposal) as the working fluids. The model is based on absorber wall temperature rather than fluid bulk temperature so it can be used to predict the performance of the collector with any working fluid. An efficiency equation for trough collectors is developed and used in a simulation model to evaluate the performance of direct steam generation collectors for different radiation conditions and different absorber tube sizes. The collector efficiency decreases with increasing feed water saturation temperature, however, the efficiency is not a strong function of operating temperature thus the maximum possible saturation temperature would be governed by costs of the pressure pipe network and balance of system cost. The collector efficiency is not significantly affected by the mode of collector operation (variable or fixed feed water flow rate), however, the pumping power due to pressure drop in the absorber tube will be different in each arrangement [21].

Su Guo et al. (2016) developed a nonlinear distribution parameter model for the dynamic behaviours of direct steam generation parabolic trough collector loops under either full or partial solar irradiance disturbance. The proposed model has shown superior performance, particularly in case of sensitivity study of fluid parameters when the pipe is partially shaded. The proposed model has been validated using experimental data from Solar Thermal Energy Laboratory of University of New South Wales, with an outlet fluid temperature relative error of only 1.91%. The validation results show that:

1. The proposed model successfully outperforms two reference models in predicting the behaviour of direct steam generation solar trough.

2. The model theoretically predicts that, during solar irradiance disturbance, the discontinuities of fluid physical property parameters and the moving back and forth of two- phase flow ending location are the reasons that result in the high-frequency chattering of outlet fluid flow.

3. The model validates that the solar irradiance disturbance at sub-cooled water region would generates larger fluctuation of fluid parameters than two phase flow region or superheated steam region [22].

Mario Biencinto et. al. (2017) simulated the behaviour of a solar thermal power plant with direct steam generation by applying the fixed and sliding-pressure strategies, and compared their annual performance in terms of electricity production. The said model had been developed in the TRNSYS software environment and reproduces the behaviour of the solar field and the power block of a 38.5 MW solar thermal power plant. They found that, during preliminary analysis at part load conditions the efficiency yields a better performance of sliding-pressure strategies with respect to the fixed-pressure case. As per the annual simulation results the use of sliding- pressure strategies

in DSG solar plants not only would allow a higher efficiency of the power block, but also would be able to provide a better solar field performance than fixed pressure due to a lower average temperature in the solar field, involving a higher amount of useful thermal energy. As a consequence, the differences in terms of annual net electricity (6.55% for constant pressure in the condenser or 7.85% for variable pressure) suggest that sliding-pressure strategies are a good way to improve the performance of DSG plants [23].

Jiangfeng Guo et. al. (2018) investigated two sensible heat storage systems and two latent heat storage systems, in which liquid lead-bismuth eutectic alloy (LBE) is selected as sensible heat storage medium and sodium nitrate is selected as phase change storage material, for concentrated solar power (CSP) with direct steam generation (DSG). They found that, for the three-tank system has higher temperature of liquid LBE in hot tank, which improves the outlet temperature of steam in discharging process. The performance of sensible heat storage system improves as the mass flow rate of water/steam increase in discharging process. For latent heat storage system the temperature difference between storage mediums and water/steam is more uniform and the outlet temperature of steam in latent heat storage is far more than that in sensible heat storage. The three-tank latent heat storage system has the most uniform temperature difference distribution among the four storage systems. Therefore, the exergy efficiency is two times more in latent heat storage system than in sensible heat storage system.Apparently, the three-tank latent heat storage system is the most flexible and efficient among the four storage systems [24].

Lu li et. al. (2017) proposed the 2D-finite volume method (FVM) and 3D-finite element volume (FEM) coupled model to conduct the thermal load and bending analysis of the heat collection element (HCE) of direct-steam-generation (DSG) PTC solar power

plant. They investigated the HCEs in evaporation and superheating stages and found that:

1. In a complete DSG loop, the HCE undergoes the highest thermal load in the superheating stage and the lowest in the evaporation stage.

2. In the evaporation stage, the stratified flow intensifies the non-uniformity of heat transfer inside the receiver tube. The wetting angle and radiation angle cooperatively affect the thermal load distribution over the HCE, further influencing the thermal bending.

3. The HCE in superheating stage withstands serious thermal load and is susceptible to the varying working condition. The factors, such as DNI and outlet temperature, have been investigated. It is found that they exert a significantly comprehensive impact on the thermal load and bending. When DNI = 1000W/m2, the circumferential temperature difference of the receiver tube is up to 48˚C and the corresponding deflection is up to 2.16 cm [25].

M. Seitz et. al. (2014) aimed to identify a complete storage concept for solar thermal power plants with direct steam generation that pays special attention to the temperature dependence of the steams specific heat capacity and at the same time allows a maximum live steam temperature during discharging. For this study, They had chosen a PCM-storage using sodium nitrate for the evaporation/condensation section of the storage system and a molten salt system for the sensible section. They found that, a significantly reduced live steam temperature can cause the reduction in power block efficiency during discharge. Furthermore, the specific storage density of the molten salt system would be reduced too [26].

J.J. Serrano-Aguilera et. al. (2014) developed a new numerical thermal model for DSG using parabolic-trough collectors. The implementation of the model has been performed from the basic governing equations and has been completely programmed in Matlab. They carried out an experimental study to validate it for 8 different operating conditions. From a fast 1-D model to solve, concerning the HTF domain, the 3-D solid domain has been worked out, evaluating thermal gradients in the steel absorber and the glass envelope. Pressure losses have also been simulated and validated. The characterization of borosilicate permits to model the radiation absorption by the solar receiver envelope, including a heat source term in the heat equation. Simulation results present a good agreement with measurements. This validated model is also useful to be solved inversely in order to get experimental heat transfer coefficients from experimental data, considering azimuthal temperature distributions [27].

Z.D. Cheng et. al. (2010) performed three-dimensional numerical simulation of coupled heat transfer characteristics in the receiver tube by combining the MCRT Method and the FLUENT software. They had chosen three typical testing conditions from the experiment to validate the physical model and simulation code; numerical results show that the predicted results agree well with the experimental data, the average relative error is within 2%. After validating the model on three typical test conditions, three models (the no-wall model, the no-radiation model and the unabridged model) are also simulated to give a further explanation of the coupled heat transfer mechanism in the receiver tube. They found that the radiation loss in Model 3 is up to 153.70W/m2. They also studied the temperature distributions of the absorber tube outer surface and the effects of direct normal irradiance, Reynolds number and emissivity of the inner tube wall on heat transfer characteristics. The Collector efficiency calculated by simulation data and collector efficiency calculated by test data agree well with each other which

also prove that the models and methods used are feasible and the numerical results are reliable [28].

D. Yogi Goswami et. al. (2013) presents a review of TES system design methodologies and the factors to be considered for CSP plants. They analysed exergy efficiency of various TES systems and Economics aspects of these systems too. They found that heat transfer mechanism and the exergy efficiency of a TES system impacts the plant level efficiency, while the cost of the system impacts the overall plant cost and energy output.

Ben Xu et. al. (2014) discussed 5 issues of technology of TES using PCM for various applications. First is about various PCM and recent development of PCM encapsulation technology. Second is the current status of research and application of latent heat storage systems in CSP plants. Third is mathematical modelling and numerical simulations. Fourth is about the issues of integration. The last one is about the cost and comparison between sensible and latent heat. They found that by developing and deploying more efficient CSP plants with TES systems, clean energy can be harnessed to power around the world [29].

G. Ram Deep et. al. (2015) experimentally analysed two PCM's namely benzamide and sebacic acid to check the compatibility of the material in solar thermal energy storage applications. The selected materials were subjected to 1000 accelerated melting and solidification cycles in order to investigate the percentage of variation at different stages on latent heat of fusion, phase transition temperature, onset and peak melting temperature. The experimental study recorded a melting temperatures of benzamide and sebacic acid as 125.09 C and 135.92 C with latent heat of fusion of 285.1 (J/g) and 374.4 (J/g). The study revealed that both benzamide and sebacic acid are potential

candidates for thermal energy storage due to their superior thermal reliability characteristics even after one thousand thermal cycles [30].

2.3 Summary of Literature reviews

It is clear from the above reviews that an ample literature is available on oRC where organic substance as working fluid have been used , the advantages of using such fluids allows them to vaporized or superheated by low or medium temperature heat sources. Many researchers have reported different fundamental thermodynamic model of ORC and have compared the thermal efficiency of different fluids. The literature indicates that the best possible thermal efficiency among the different presented model for varying expander and condensation temperatures. The highest thermal efficiency range (9.8%-13.4%) was obtained when used to heat exchanger and feed water heater. It is also concluded that R245fa has potential working fluid for ORC applications, especially for those with low to medium temperature heat sources.

2.4 Literature Gap

From the above referred literature this is cleared that limited work has been done in calculation of the exergetic efficiency, also there is not much literature is available on the same using different types of organic Rankine cycle with HFE7000 and HFE7100. No work has been done on superheated cycle, with feed water heater and also for internal heat exchanger in ORC.

2.5 Objective

The objective of the present research work is

1. To find the thermodynamic efficiency for R245fa, HFE7100 and HFE7000 in organic Rankine cycle with IHE, saturated cycle and organic Rankine cycle with feed water heater.

2. To compute the exergetic efficiency of ORC for saturated, ORC with feed water heater and ORC with heat exchanger for the fluids like R245fa, HFE7100 and HFE7000.

CHAPTER 3

THERMODYNAMIC MODELLING

3.1 Introduction

The basic simulation is been done on the four component such as expander, condenser, evaporator and pump. Here in this basically the variation of expander temperature is seen over the cycle efficiency , same as for the evaporator temperature in first part . In second part I will go for the exergy destruction where while changing the fluid of resembling properties also whose critical point are merely equal or nearby are compared. Here in this I have taken R245fa, HFE7000 and HFE7100.

3.1.1 Basic ORC model

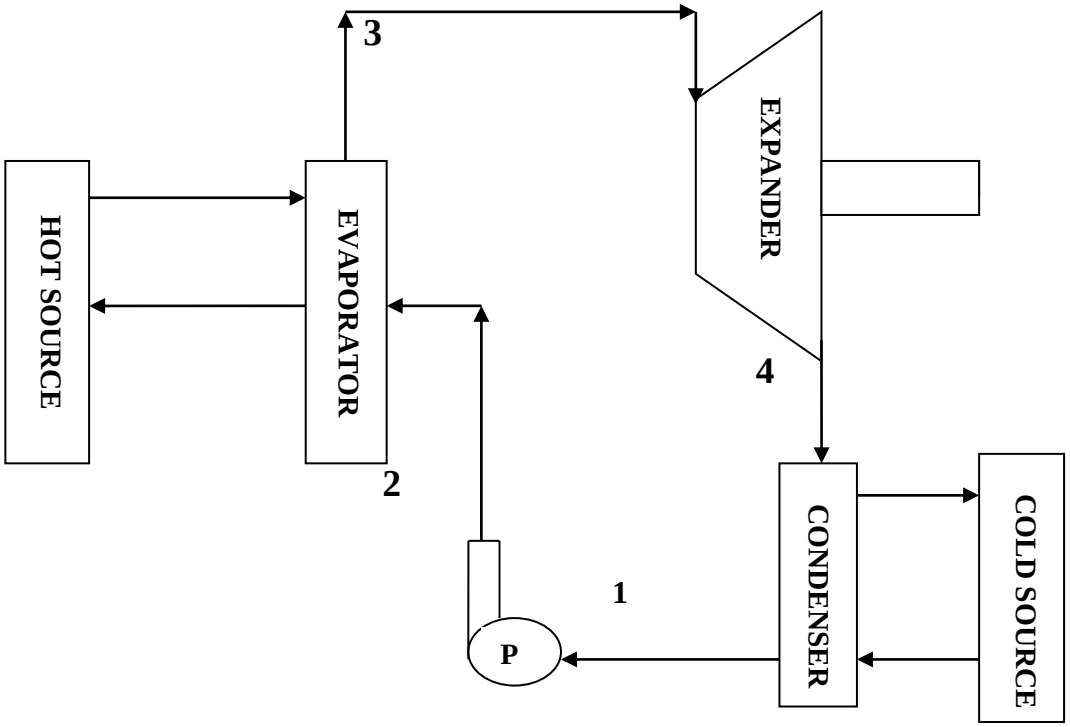

Figure 10: Basic model of ORC

The operating principles of Rankine cycle and organic Rankine cycle is merely same, just the difference is there in the fluid in Rankine cycle water or steam is circulated over the cycle i.e evaporation and condensation take place . In case of oRC , fluid used is organic fluid. The methodology goes like this, the effective fluid, which occurs originally into a liquid state is feed through the pump into the evaporator at appropriate delegated pressure and mass flow rate. The effective fluid is warmed to the designated temperature level within the evaporator where the fluid accomplishes a tremendous temperature and is then with large pressure and temperature of the evaporator goes to turbine where the expansion take place and rotational power is produced. Then the low pressurized fluid is condensed in the condenser to the liquid state before it is again circulated in the pump. here in condenser the dissipation of heat to the surrounding take place.

The thermodynamic ORC models were examined in aforementioned study of three different fluid that are R245fa, HFE7000, HFE7100. In order to get the best suited result for the path T-S diagrams of different types are drawn in Fig.11, Fig.12, Fig.13.

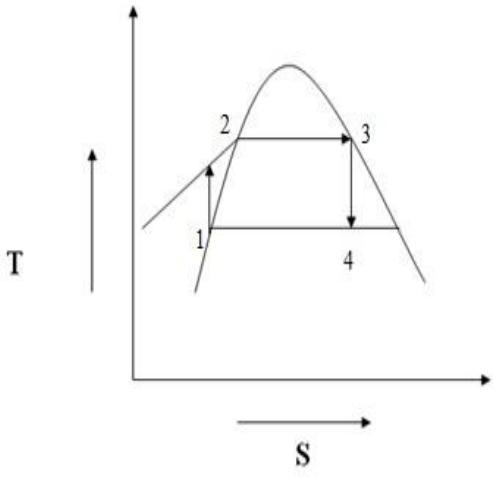

Figure 11: T-s for saturated ORC with wet fluid

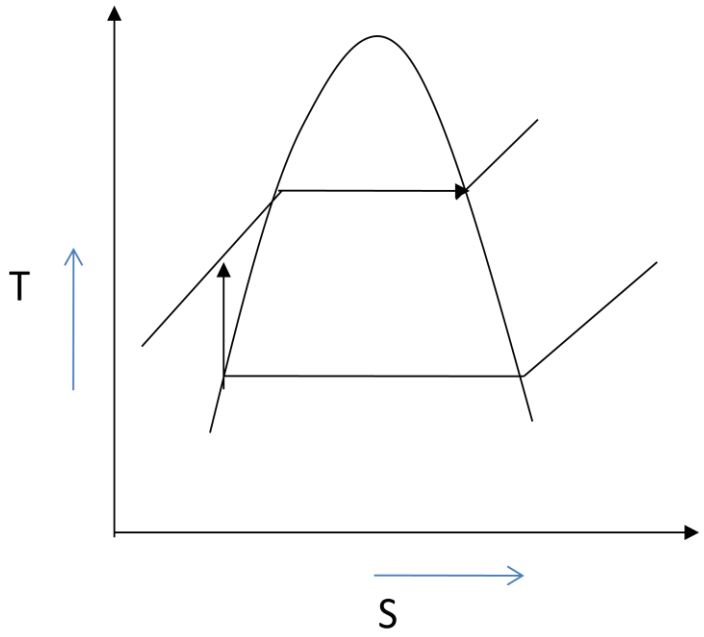

Figure 12 : T-s for trilateral ORC with dry fluid

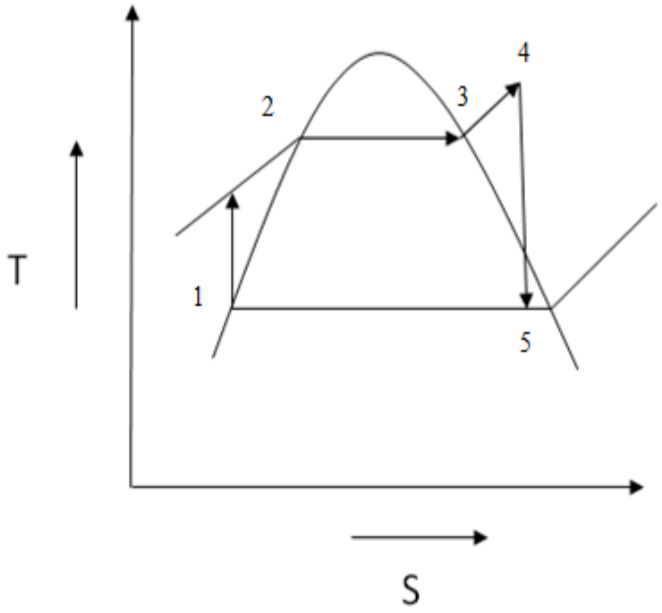

Figure 13 : T-s for superheated ORC with isentropic fluid

3.2 EXERGY ANALYSIS

The exergy from the system at a given state can be defined as the greatest work which can be extricated of it to accomplished the thermodynamic stability with the surrounding. It is a very vital concept in all energy- composing, energy-devouring and energy-conducting systems. The second order indicates that all classes of energy are not the related attributes and the degree of energy constantly diminishes while preserving its quantity.

$$ED_i = \sum(\boldsymbol{me})_{\boldsymbol{in}} - \sum(\boldsymbol{me})_{\boldsymbol{out}} + [\sum(\boldsymbol{Q}(\mathbf{1} - \frac{\boldsymbol{T_o}}{\boldsymbol{T}})_{in}) + \sum(\boldsymbol{Q}(\mathbf{1} - \frac{\mathbf{T_o}}{\boldsymbol{T}})_{out})] \pm \sum \boldsymbol{W} \quad (3.2.1)$$

where EDi depicts the percentage of exergy destruction transpiring in the method in the segment under deliberation.

The initial expressions on the right represent the exergy of streams subscribing and transmitting the command volume from fig.10. The third and fourth expressions are the exergy linked with heat transferal Q from the reservoir sustained at a consistent temperature 'T' and are equal to work received by Carnot engine operating within 'T' and 'To'. The latter expressions are the mechanical work transmitted to or from the control volume. Second law enforcement of the system can be estimated in expressions of exergetic efficiency where 'Tr' is the temperature of the area to be moderated. Exergetic efficiency can similarly be represented in terms of cumulative exergy destruction and exergy furnished to the system i.e. the exergetic efficiency shows the rate of the combustible exergy contributed to a system that is found in the product exergy.

Exergy destruction in evaporator:

$$Ed_{evp}=(h_2-T_o*S_2)-(h_3-T_o*S_3)+Q_s*[1-\frac{T_o}{T_h+273}] \quad (3.2.2)$$

Exergy destruction in expander:

$$Ed_{exp}=(h_3-T_o*S_3)-(h_4-T_o*S_4)-(h_3-h_4) \quad (3.2.3)$$

Exergy destruction in condenser:

$$Ed_{cond}=(h_4-T_o*S_4)-(h_1-T_o*S_1) \quad (3.2.4)$$

Exergy destruction in pump:

$$Ed_{pump}=(h_1-T_o*S_1)-(h_2-T_o*S_2)+(h_2-h_1) \quad (3.2.5)$$

Exergetic Efficiency:

$$\eta_{ex}=1-\frac{Ed_{total}}{E_{input}} \quad (3.2.6)$$

$$E_{input}=Q_s*[1-\frac{(T_o)}{(T_h+273)}]+W \quad (3.2.7)$$

$$\eta_{ex1}=\frac{W_t}{E_{input}} \quad (3.2.8)$$

3.3 INPUT CONDITION

The input to the thermodynamic model of the organic Rankine cycle are as follows:

Fixed expander isentropic efficiency ($\eta_T = 0.80$) and fixed pump isentropic efficiency ($\eta_P = 0.60$)

The thermodynamic properties of various working fluids at different points are calculated using EES programs.

The values given in the table are referred from following reference [8].

Cycle	Expander temperature (˚C)	Condenser temperature(˚C)	Fluids used
Saturated cycle	80-120	30	R245fa, HFE7000 and HFE7100
ORC with feed water heater	80-150	30	
ORC with heat exchanger	80-150	20	

CHAPTER 4

RESULT AND DISCUSSION

This chapter deal with the result and discussion of various cycles with different organic fluids at different expander inlet temperature, fixed condenser temperature . In this the first law of efficiency is calculated and also the exegetic efficiency and there comparison is done to come to stimulated result.

4.1 THERMODYNAMIC EFFICIENCY FOR DIFFERENT CYCLE

4.1.1 Saturated Cycle:

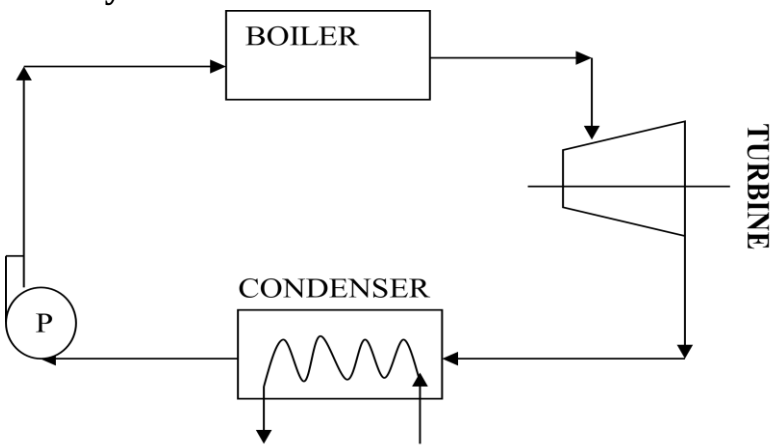

Figure 14: Block diagram of saturated cycle

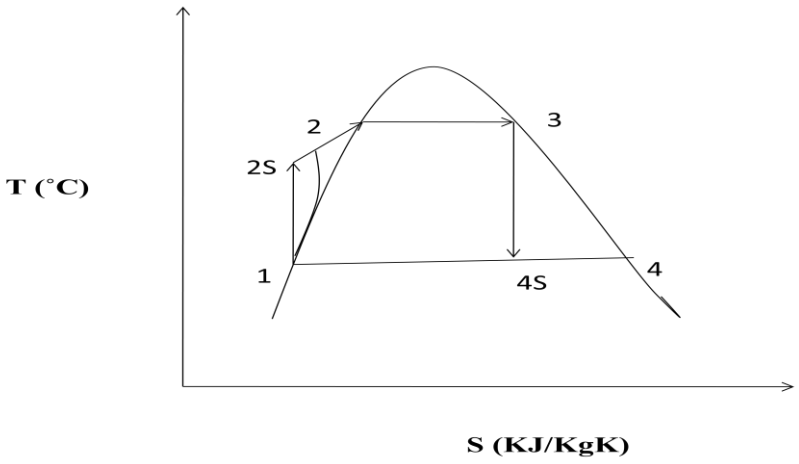

Figure 15: T-s diagram of saturated cycle

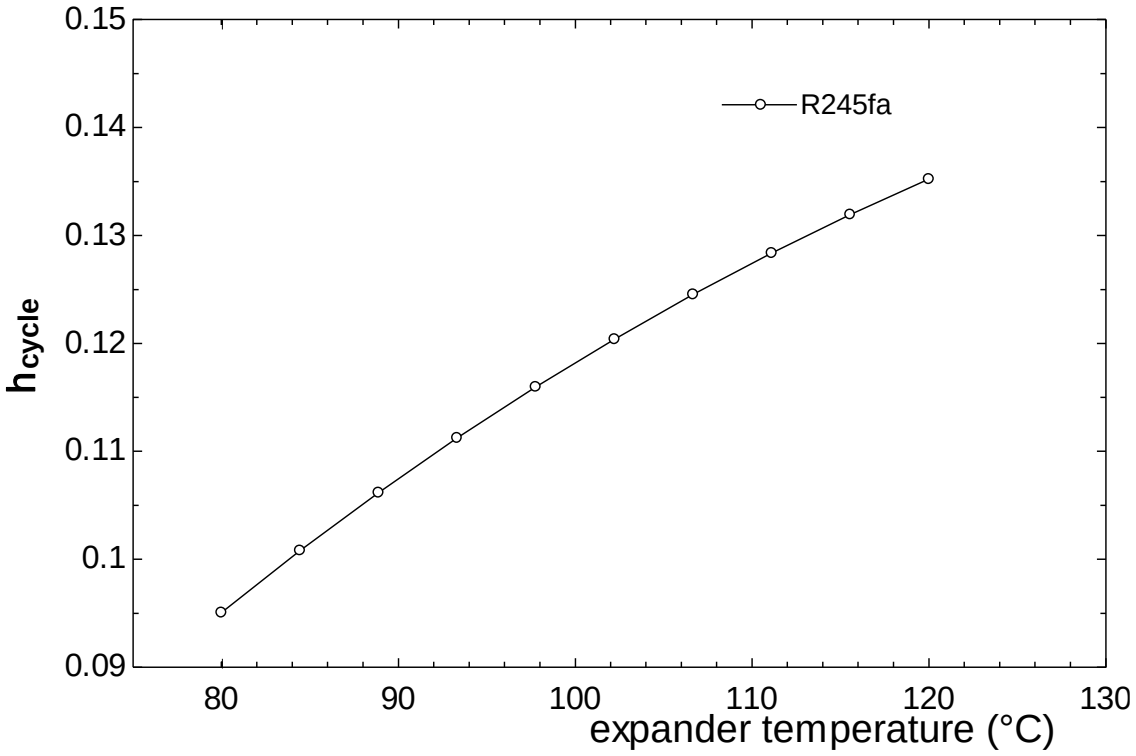

Figure 16: thermal efficiency for saturated cycle with R245fa

Above figure shows the increase in the efficiency of the cycle with increase in the expander inlet temperature. Here the efficiency of the pump and the turbine are taken at 0.60 and 0.80 respectively. There is a gradual increase in the performance of cycle for the fluid R245fa. The variation of temperature is from 80-130˚C and the change in the efficiency is from 0.09 to 0.14.

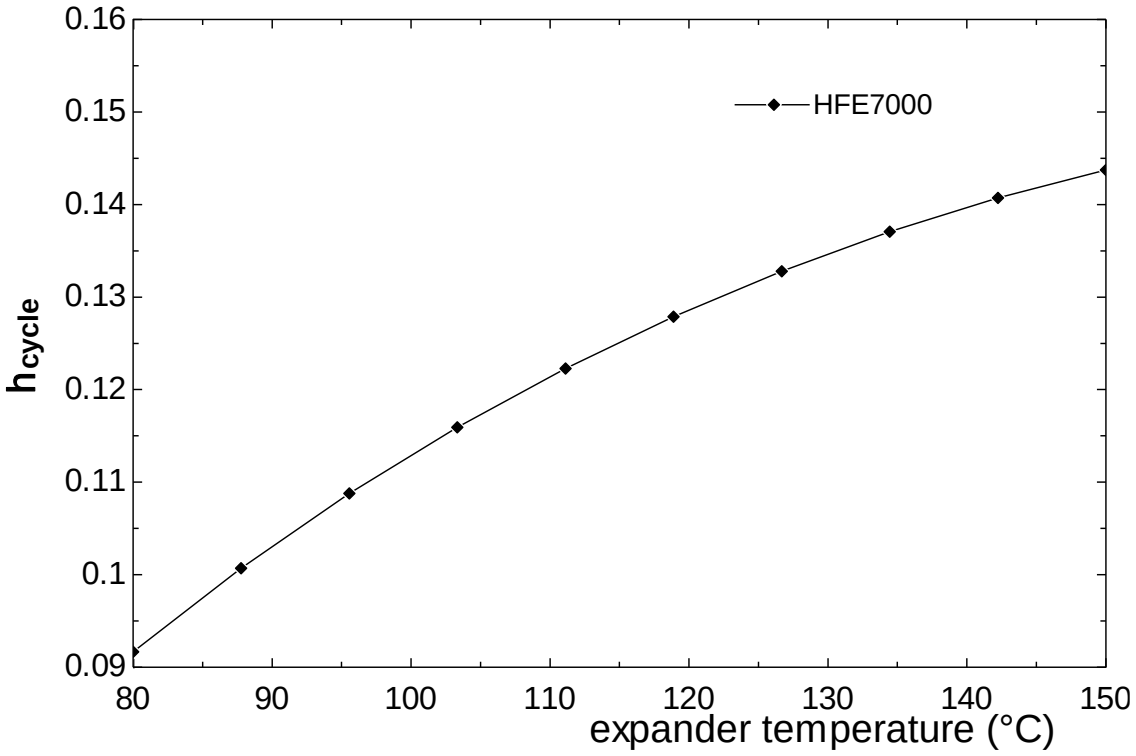

Figure 17: thermal efficiency for saturated cycle with HFE7000

Above figure show the increase in the efficiency of the cycle with increase in expander inlet temperature. Here efficiency of pump also turbine efficiency are taken as 0.60 and 0.80 respectively. There is gradual increase in efficiency of cycle for the fluid HFE7000. The variation of temperature is from 80-150˚C and the change in the efficiency is from 0.9 to 0.145.

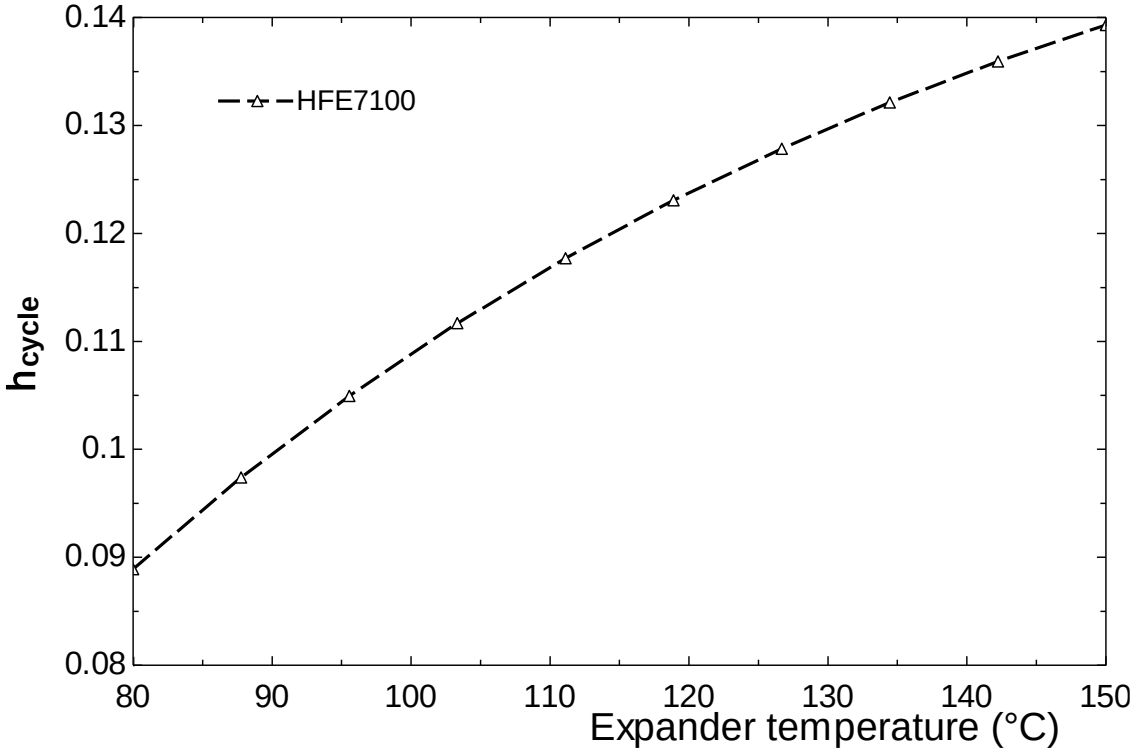

Figure 18: thermal efficiency for saturated cycle with HFE7100

Above figure show the increase in the efficiency of the cycle with gradual increase in expander inlet temperature. Here efficiency of pump also turbine efficiency are taken as 0.60 and 0.80 respectively. There is gradual increase in efficiency of cycle for the fluid HFE7100. The variation of temperature is from 80-150˚C and the change in the efficiency is from 0.9 to 0.14.

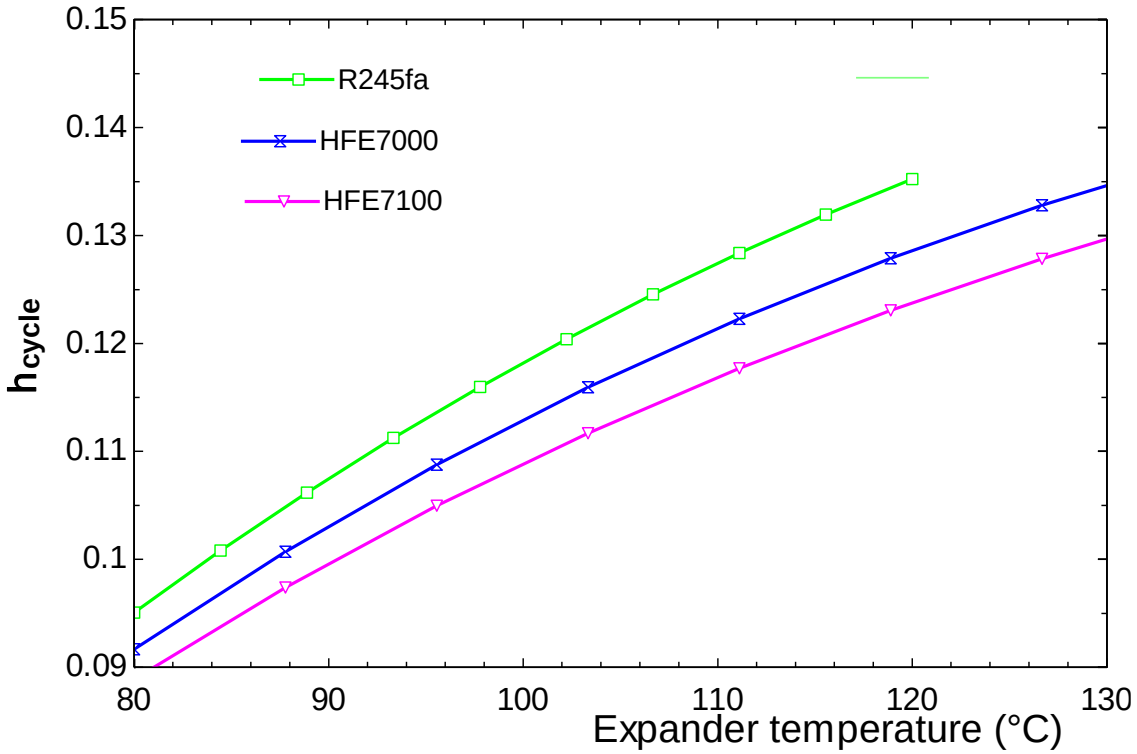

Figure 19: comparison of thermal efficiency of saturated cycle with R245fa, HFE7000 and HFE7100

Above figure show the comparison in the efficiency of the cycle after the increase in expander entering temperature. Here efficiency of the pump also the turbine efficiency are taken as 0.60 and 0.80 respectively. There is gradual increase in the efficiency of cycle for the fluid R245fa. The variation of temperature is from 80-130˚C and the change in the efficiency is from 0.9 to 0.12. Maximum efficiency is for R245fa.

4.1.2 Regeneration In Organic Rankine Cycle :

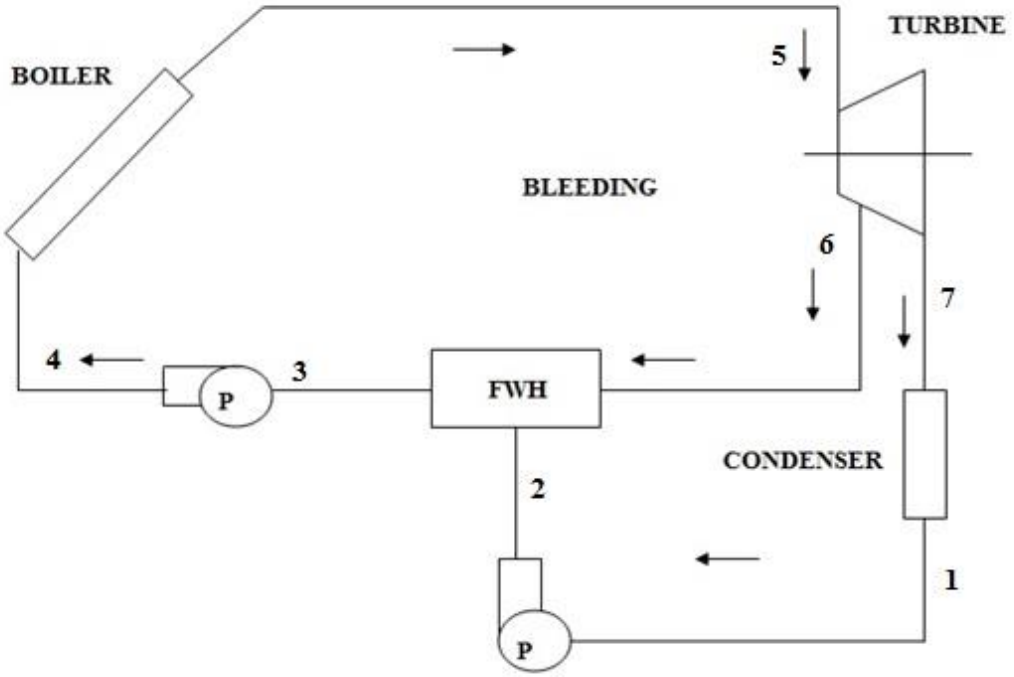

Figure 20: Regeneration in organic Rankine cycle

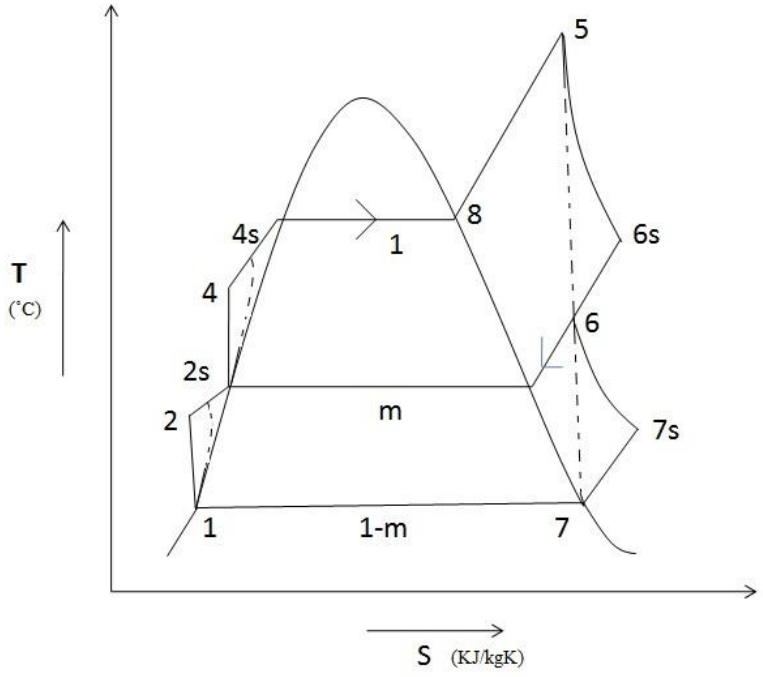

Fig.21: T-s diagram of organic Rankine cycle with feed water heater

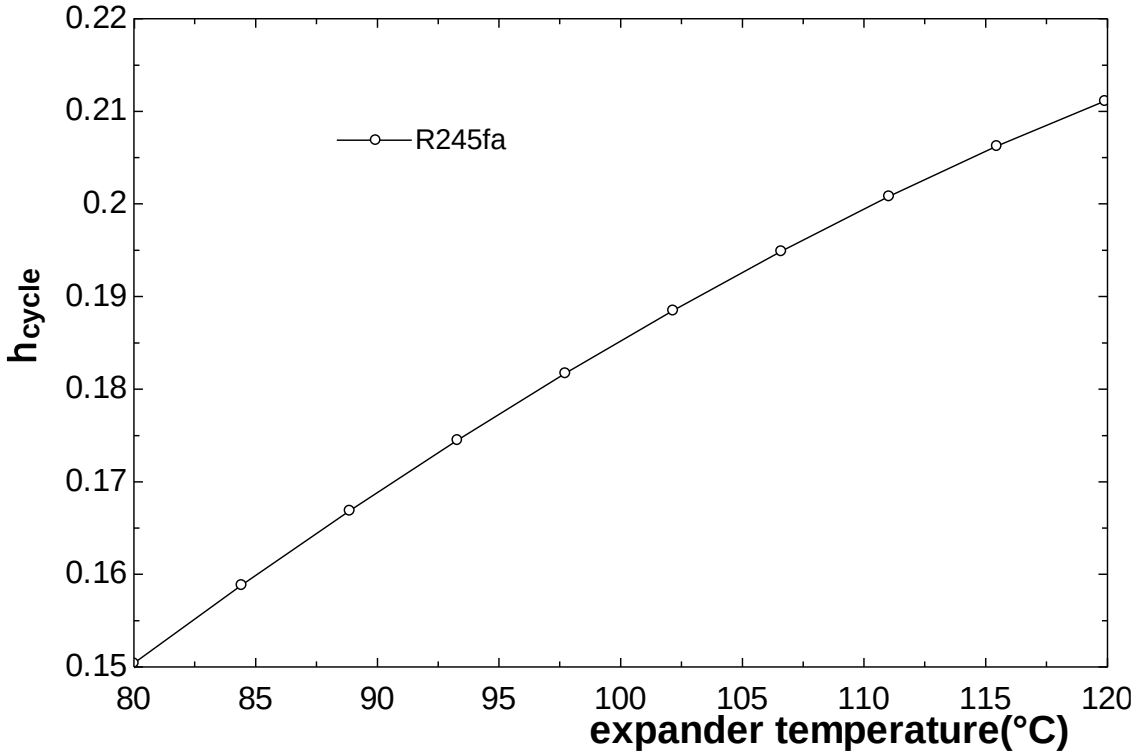

Fig. 22: thermal efficiency for regeneration cycle with R245fa

Above figure show the increase in the efficiency of the cycle with increase in expander entering temperature. Here the efficiency of pump also the turbine efficiency are taken as 0.60 and 0.80 respectively. There is gradual increase in the efficiency of cycle for the fluid R245fa. The variation of temperature is from 80-130˚C and the change in the efficiency is from 0.15 to 0.21.

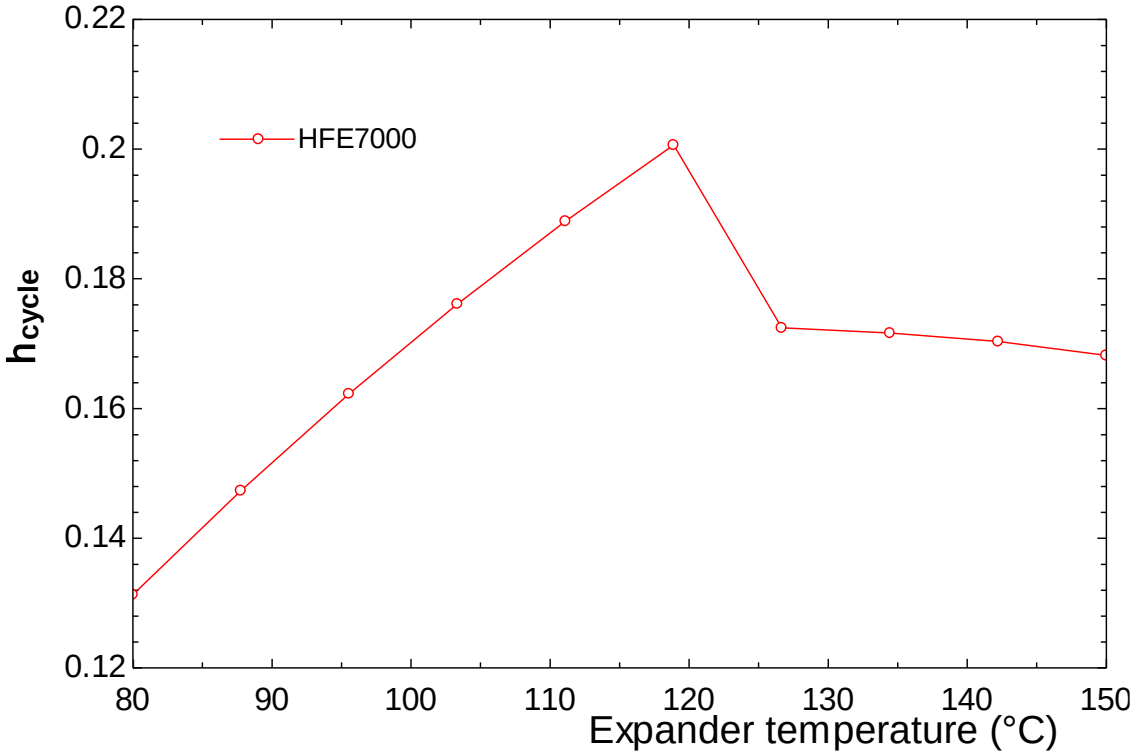

Figure 23: thermal efficiency for regeneration cycle with HFE7000

Above figure show the increase in the efficiency of the cycle with increase in the expander in-let temperature. Here the efficiency of pump & the turbine are taken as 0.60 and 0.80 respectively. There is gradual increase in the efficiency of cycle for fluid HFE7000. The variation of temperature is from 80-150˚C and the change in the efficiency is from 0.13 to 0.2, then after that for 130-150˚C , the efficiency is 0.18.

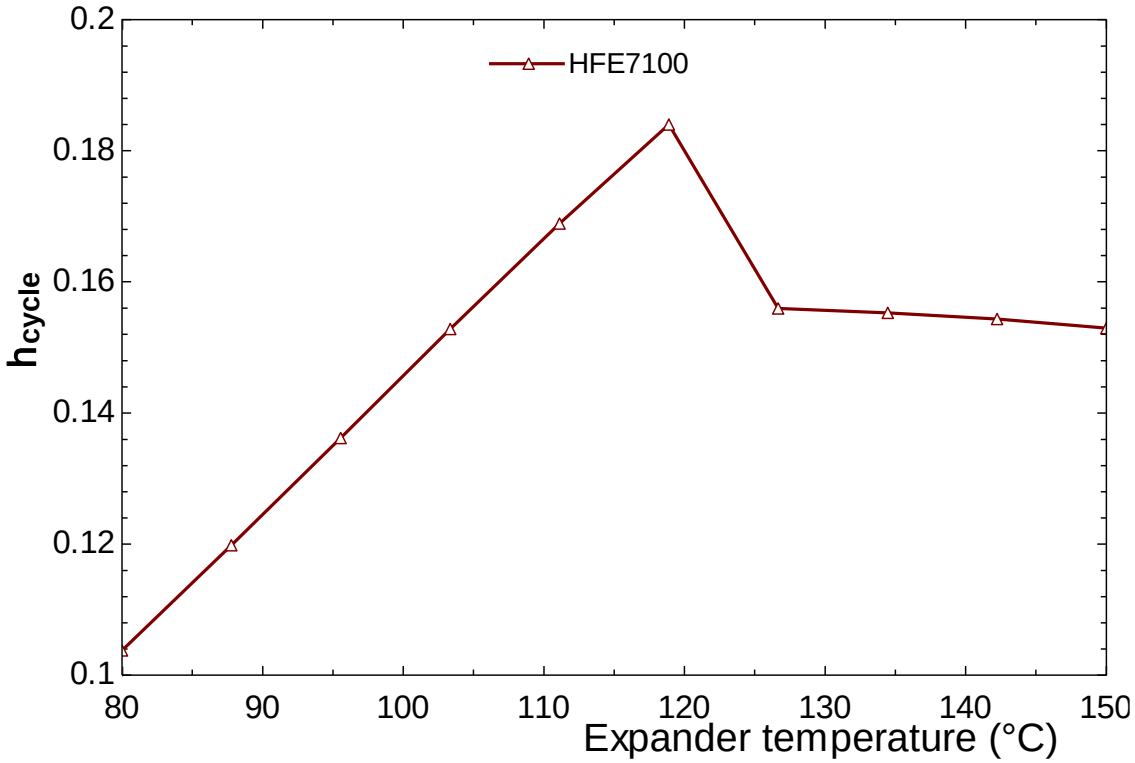

Figure 24: thermal efficiency for regeneration cycle with HFE7100

Above figure shows the increase in efficiency of cycle with increase in expander inlet temperature. Here efficiency of pump and turbine are taken as 0.60 and 0.80 respectively. There is gradual increase in the efficiency of cycle for fluid HFE7100. The variation of temperature is from 80-150˚C and the change in the efficiency is from 0.1 to 0.18, after that gradual decrease than 0.16.

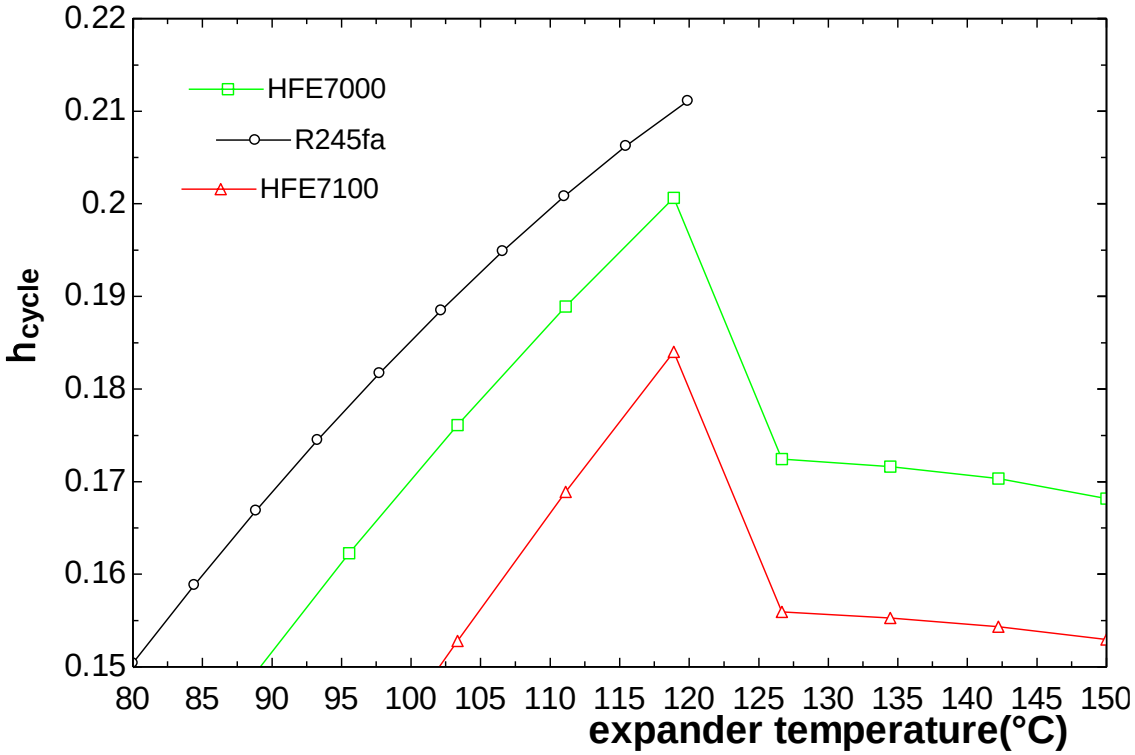

Figure 25: Comparison of thermal efficiency of regeneration cycle with R245fa, HFE7000 and HFE7100

Above figure show the comparison in efficiency of cycle with increase in expander in-let temperature. Here efficiency of pump and turbine_efficiency are taken as 0.60 and 0.80 respectively. There is gradual increase in efficiency of the cycle for fluid R245fa, HFE7000 and HFE7100. The variation of temperature is from 80-150˚C and the change in the efficiency is from 0.15 to 0.21. Maximum is for R245fa.

4.1.3 Organic Rankine Cycle With Heat Exchanger:

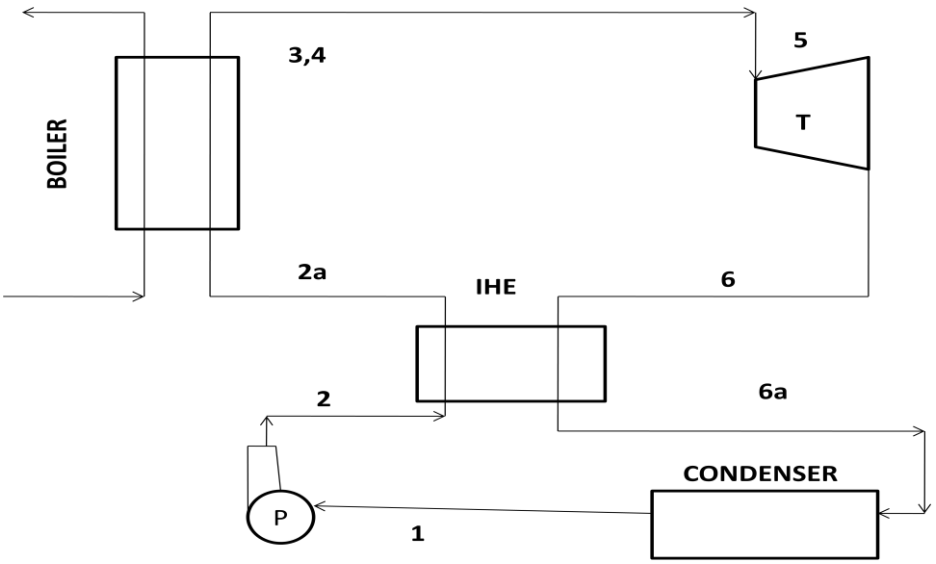

Figure 26: Block diagram of ORC with IHE

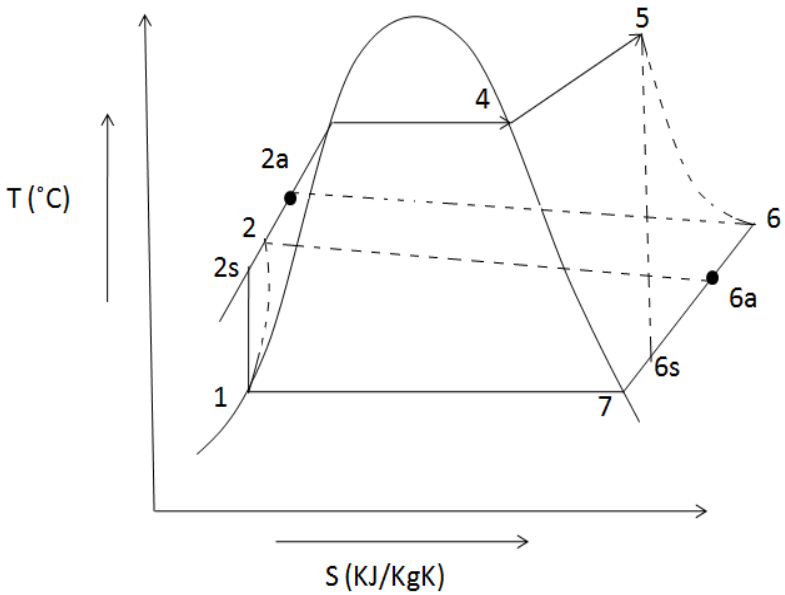

Figure 27: T-s diagram for organic Rankine cycle with heat exchanger

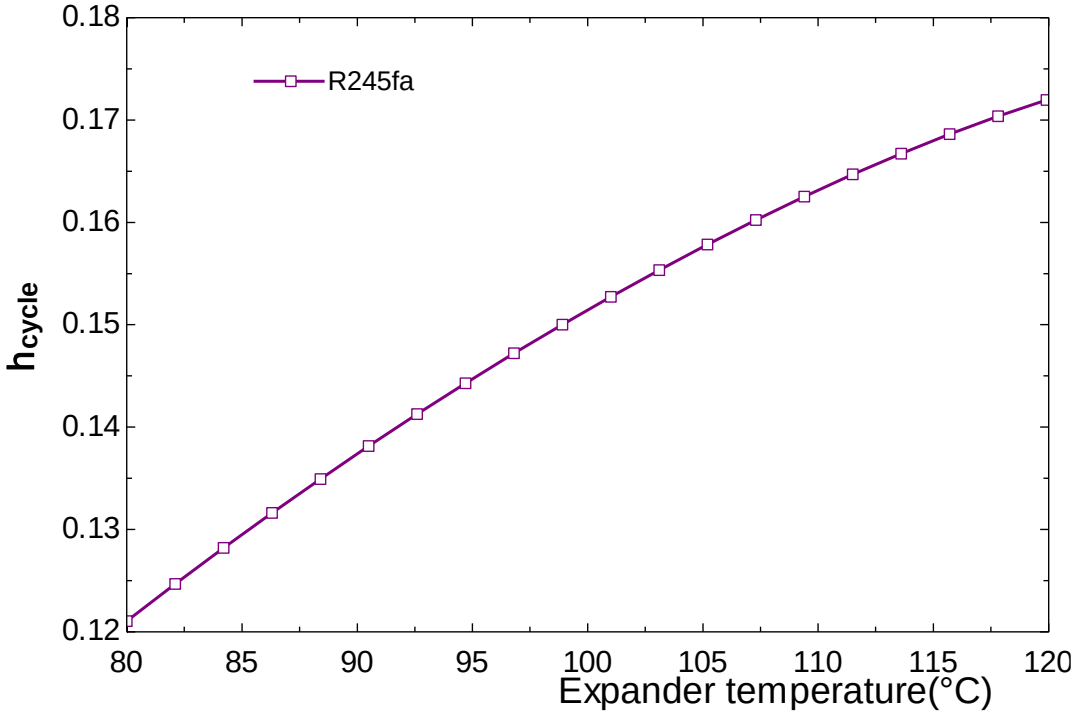

Figure 28 : thermal efficiency for ORC with heat exchanger with R245fa

Above figure show the increase in efficiency of cycle with increase in expander inlet temperature. Here efficiency of pump and of turbine are taken as 0.60 and 0.80 respectively. There is gradual increase in efficiency of cycle for the fluid R245fa. The variation of temperature is from 80-120˚C and the change in the efficiency is from 0.12-0.17. Here due to the use heat exchanger the wet fluid is heated again that make it efficient as wear-tear reduced in turbine.

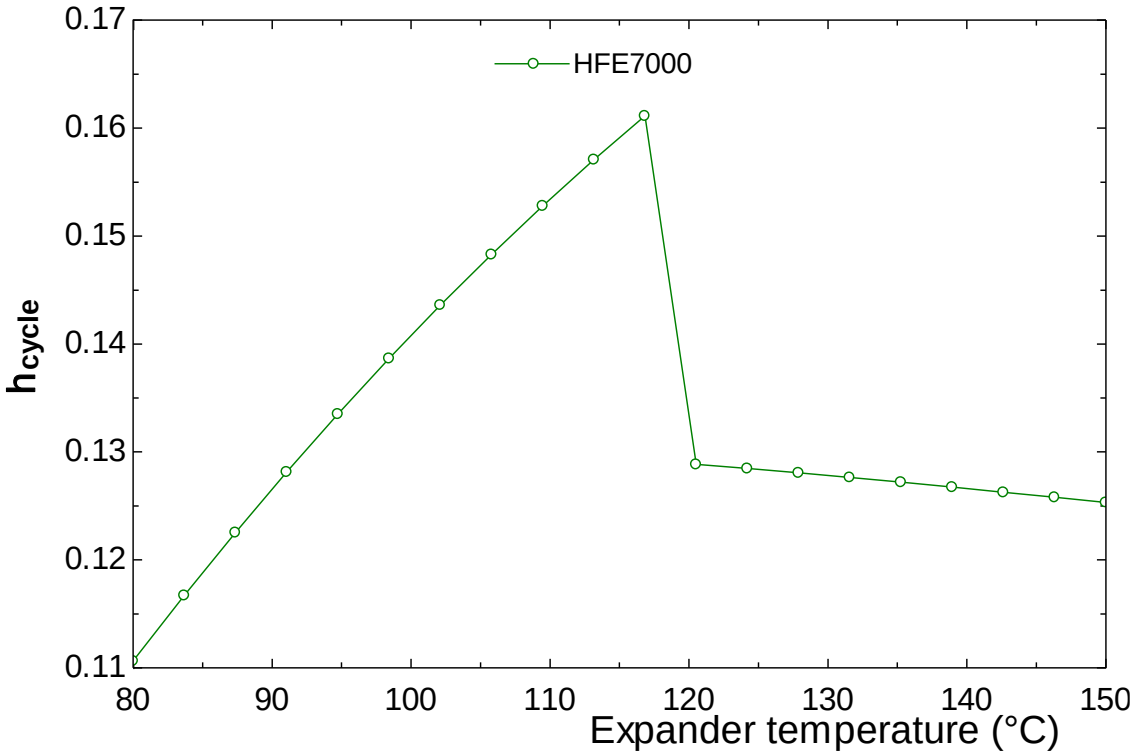

Figure 29: thermal efficiency for ORC with heat exchanger with HFE7000

Above figure show the increase in efficiency of cycle with increase in expander inlet temperature. Here the efficiency of pump and of turbine are taken as 0.60 and 0.80 respectively. There is gradual increase in efficiency of cycle for the fluid HFE7000. The variation of temperature is from 80-120˚C and after that there is gradual decrease in efficiency and then same variation can be seen been 120-150˚C. the change in the efficiency is from 0.11 to 0.16, after that 0.135-0.130.

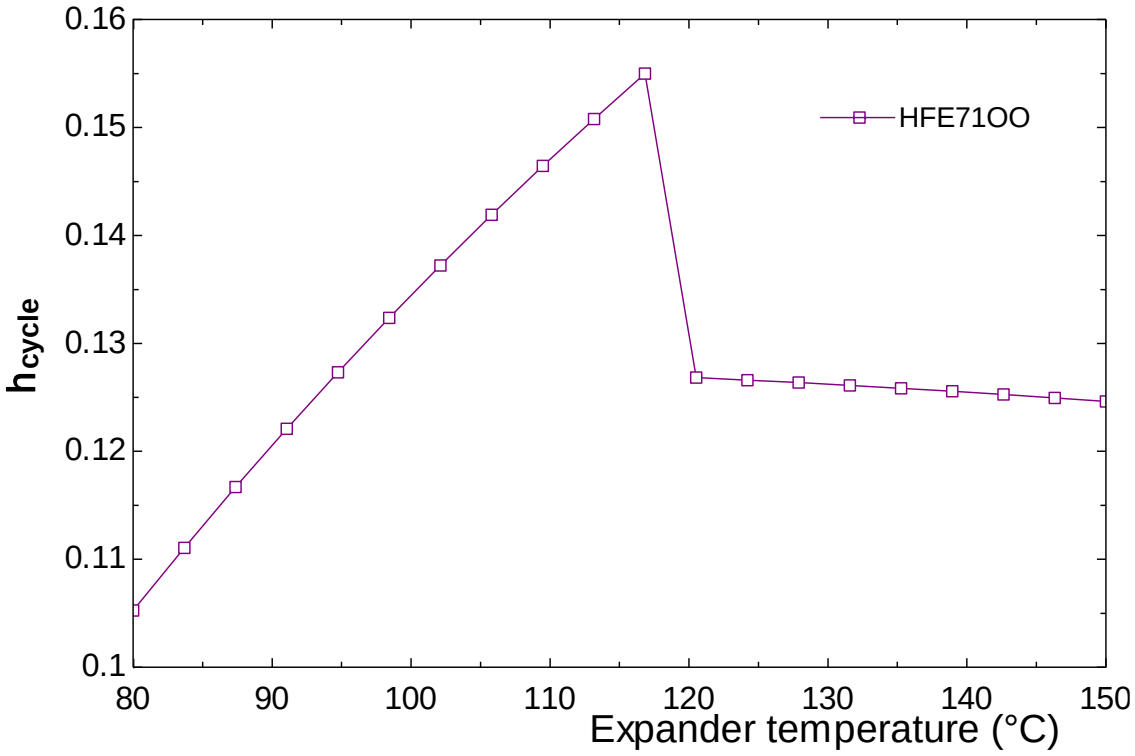

Figure 30 : thermal efficiency for ORC with heat exchanger with HFE7100

Above figure show the increase in efficiency of cycle with increase in expander inlet temperature. Here the efficiency of the pump and the turbine are taken as 0.60 and 0.80 respectively. There is gradual increase in efficiency of cycle for the fluid HFE7100. The variation of temperature is from 80-150˚C and the change in the efficiency is from 0.11 to 0.155, after that gradual decrease and then constant from 0.12-0.115.

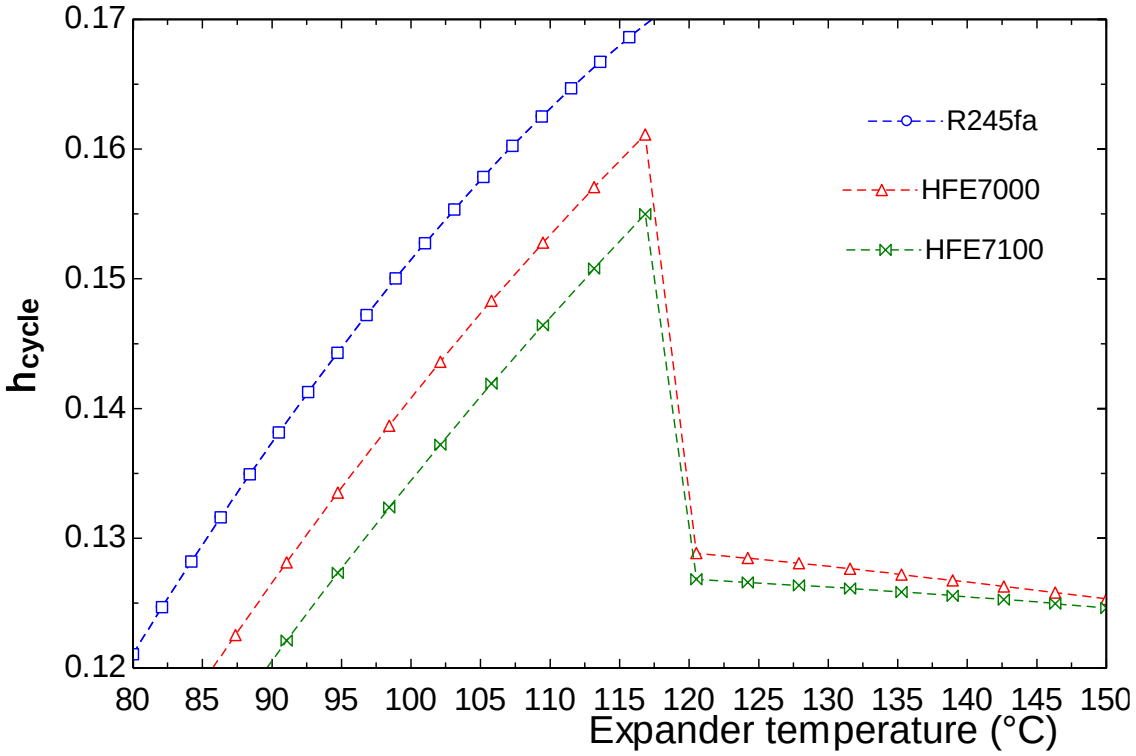

Figure 31 : comparison of thermal efficiency for oRC with heat exchanger with R245fa, HFE7100 and HFE7000

Above figure show the comparison between the efficiency of the cycle with increase in expander inlet temperature. Here the efficiency of pump and of turbine are taken as 0.60 and 0.80 respectively. There is gradual increase in the efficiency of cycle for fluid R245fa. The variation of temperature is from 80-150˚C and the change in the efficiency is from 0.12-0.17. Maximum efficiency is for R245fa.

4.2 EXERGETIC ANALYSIS

4.2.1 Saturated Cycle

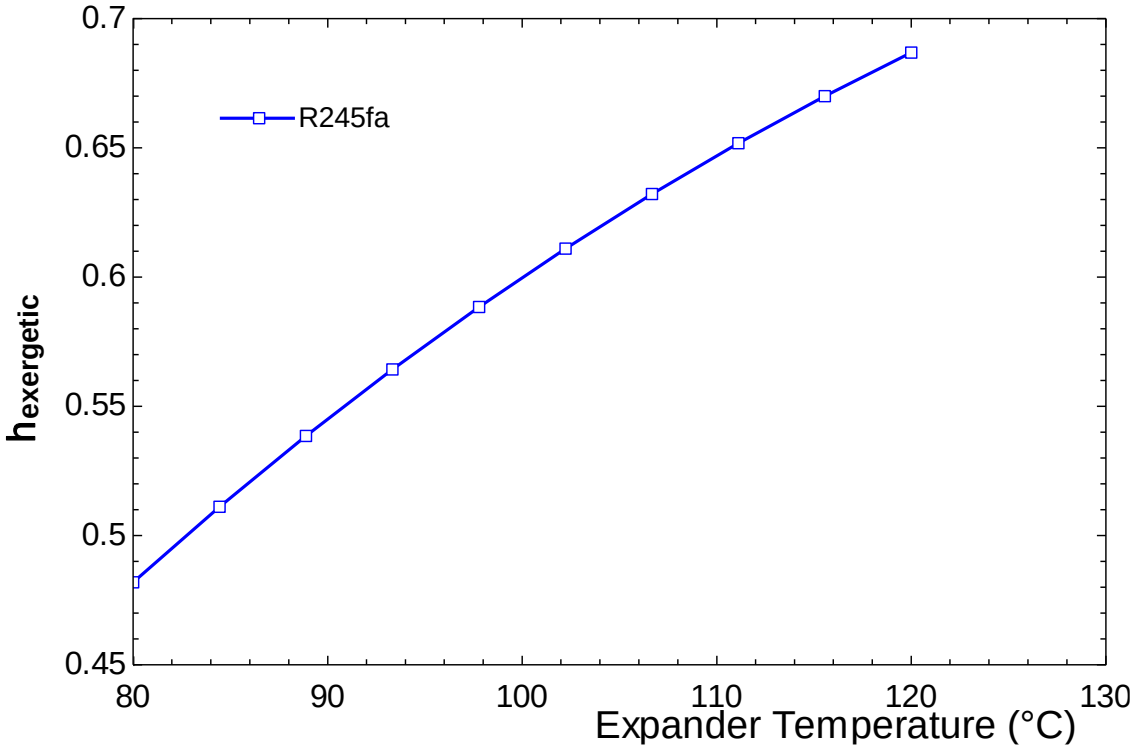

Figure 32: Exergetic Efficiency of Saturated Cycle With R245fa

Above figure show the incremental increase of exergetic efficiency of cycle with increase in the expander entering temperature. Here efficiency of pump and of turbine are taken as 0.60 and 0.80 respectively. There is gradual increase in the efficiency of cycle for fluid R245fa. The variation of temperature is from 80-130˚C and the change in the exergetic efficiency is from 0.4 to 0.67.

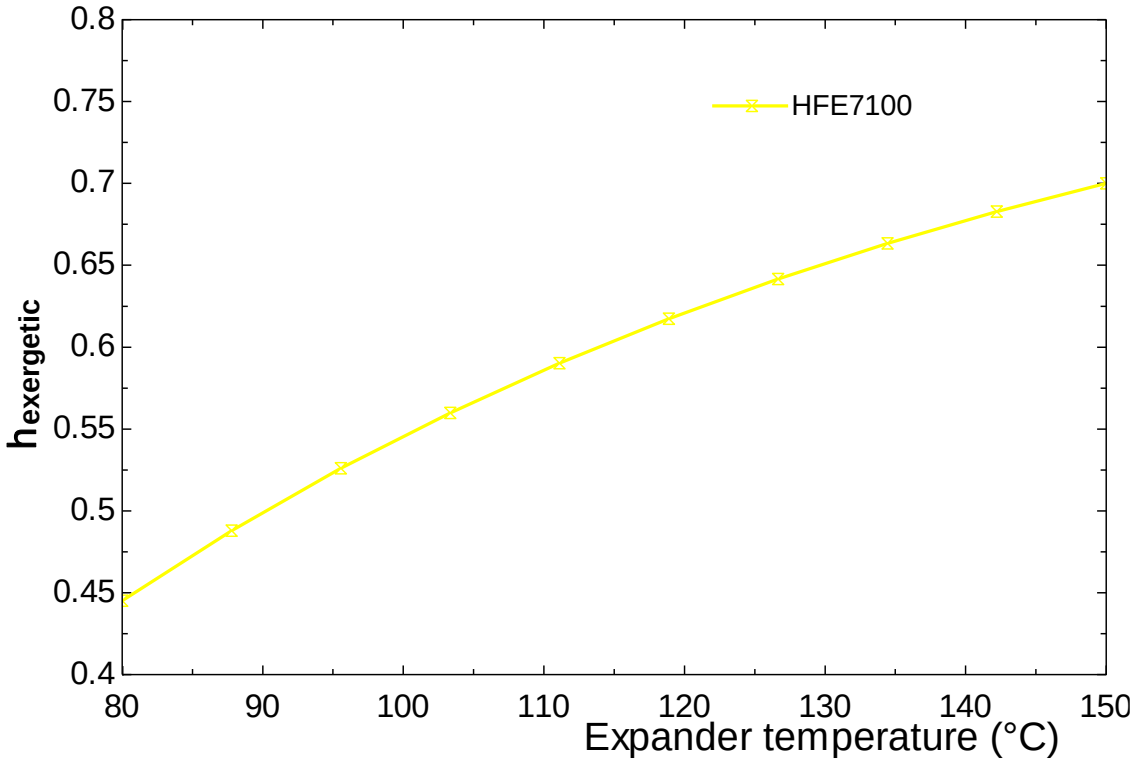

Figure 33: Exergetic Efficiency of Saturated Cycle With HFE7100

Above figure shows the incremental increase of exergetic efficiency of the cycle with increase in expander inlet temperature. Here the efficiency of pump and turbine are taken as 0.60 and 0.80 respectively. There is gradual increase in the efficiency of cycle for fluid R245fa. The variation of temperature is from 80-150˚C and the change in the exergetic efficiency is from 0.45 to 0.7.

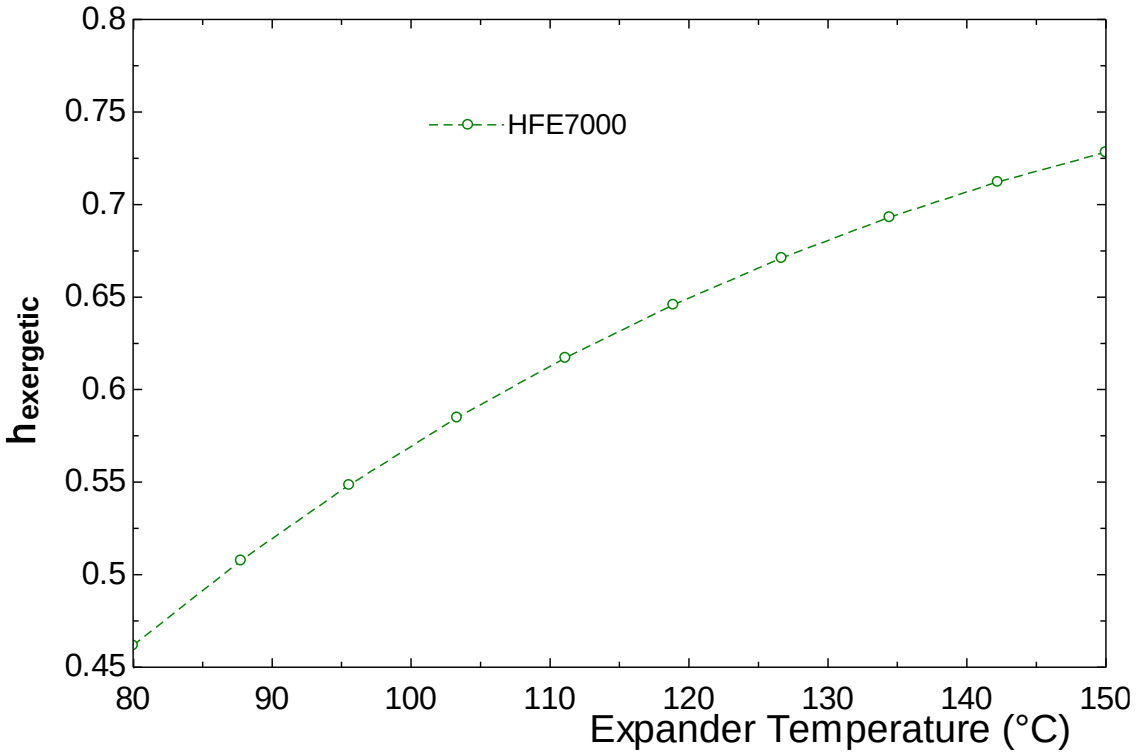

Figure 34: Exergetic Efficiency of Saturated Cycle With HFE7000

Above figure shows incremental increase of exergetic efficiency of cycle with increase in expander in-let temperature. Here efficiency of pump and turbine are taken as 0.60 and 0.80 respectively. There is gradual increase in efficiency of cycle for the fluid R245fa. The variation of temperature is from 80-150˚C and the change in the exergetic efficiency is from 0.45 to 0.725.

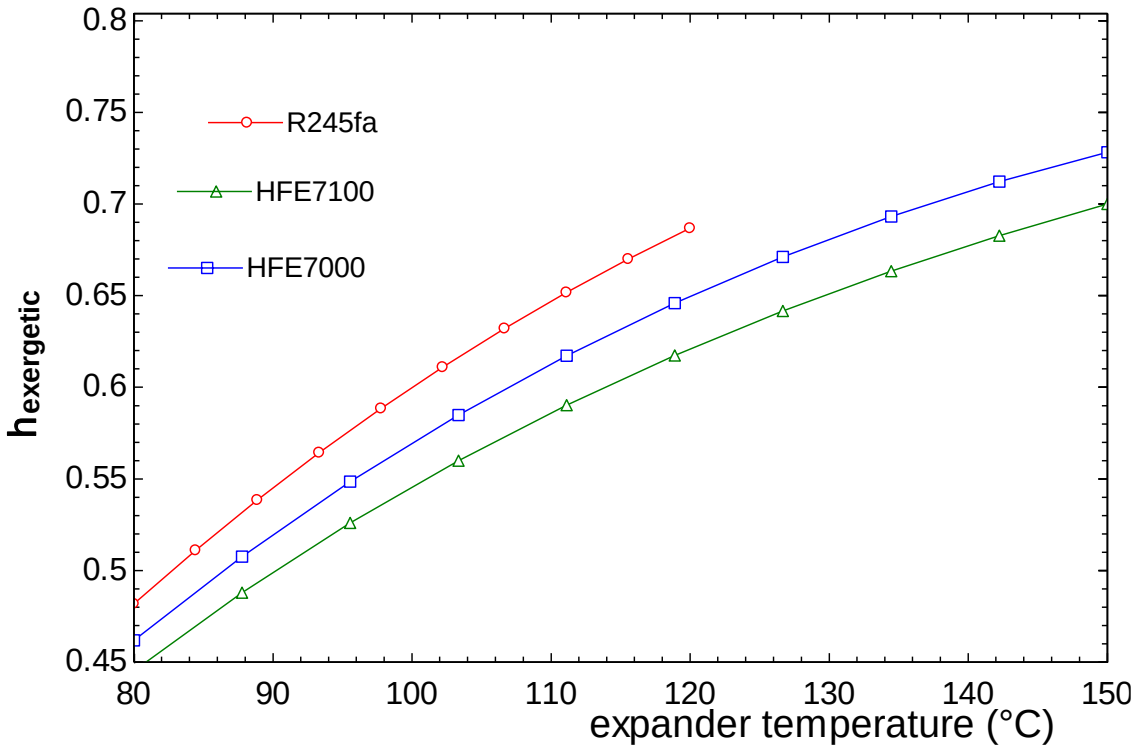

Figure 35: comparison of Exergetic Efficiency of Saturated Cycle With R245fa, HFE7000 and HFE7100

Above figure show comparison of increase in the exergetic efficiency of cycle with fluids like R245fa, HFE7000and HFE7100 with increase in expander inlet temperature. Here efficiency of pump and turbine are taken as 0.60 and 0.80 respectively. There is gradual increase in efficiency of cycle for fluid R245fa, HFE7000and HFE7100. The variation of temperature is from 80-150˚C and the change in the exergetic efficiency is from 0.45 to 0.725 for HFE7100 , 0.45 to 0.7 for R245fa and 0.3 to 0.675 for HFE7000.

4.2.2 Regeneration in ORC :

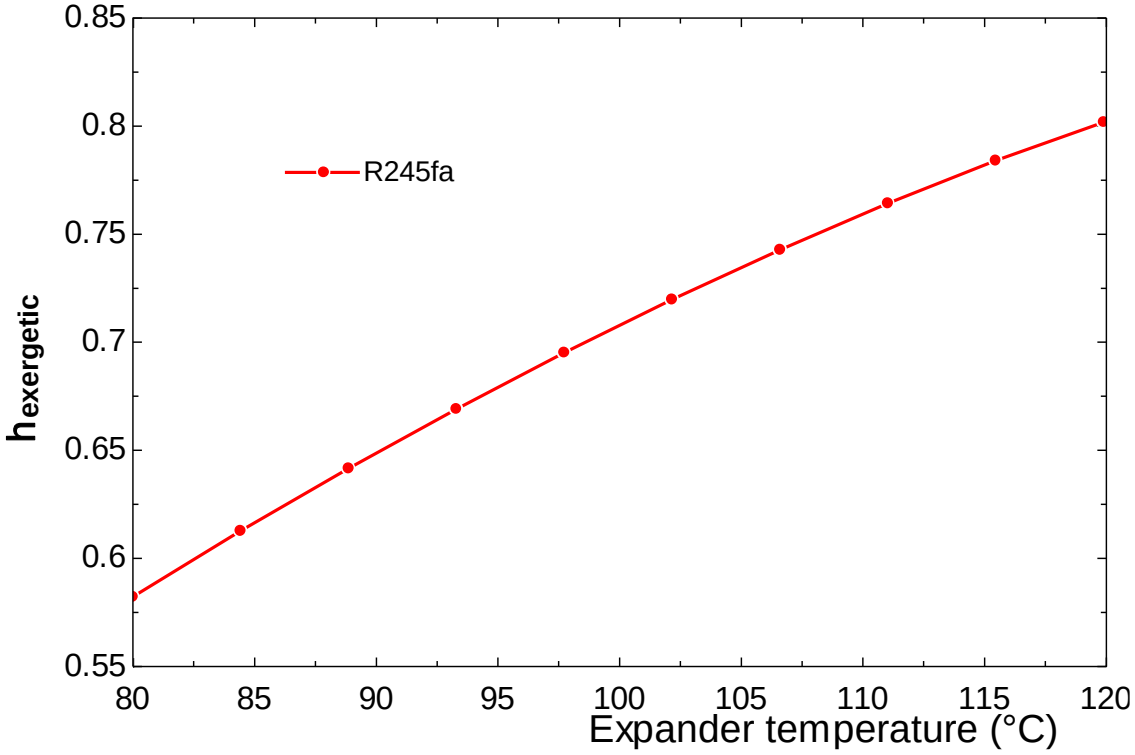

Figure 36: Exergetic Efficiency of regeneration Cycle With R245fa

Above figure show the incremental increase of exergetic efficiency of regeneration cycle with increase in the expander inlet temperature. Here the efficiency of pump and turbine are taken as 0.60 and 0.80 respectively. There is gradual increase in efficiency of cycle for the fluid R245fa. The variation of temperature is from 80-120˚C and the change in the exergetic efficiency is from 0.60 to 0.8

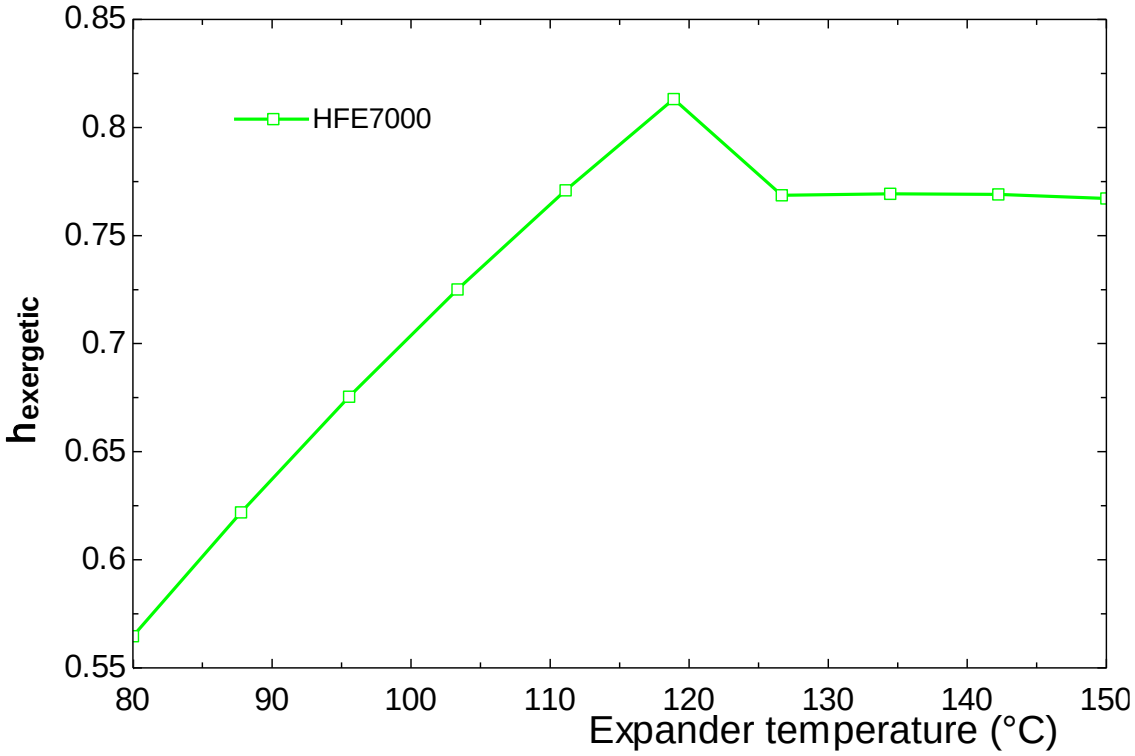

Figure 37: Exergetic Efficiency of regeneration Cycle With HFE7000

Above figure show the incremental increase of exergetic efficiency of regeneration cycle with increase in expander inlet temperature. Here efficiency of pump and turbine are taken as 0.60 and 0.80 respectively. There is gradual increase in efficiency of cycle for fluid HFE7000. The variation of temperature is from 80-150˚C and the change in the exergetic efficiency is from 0.55 to 0.8 till 120˚C and after that gradual decrease then from 130-150˚C gradually the same efficiency of 0.775.

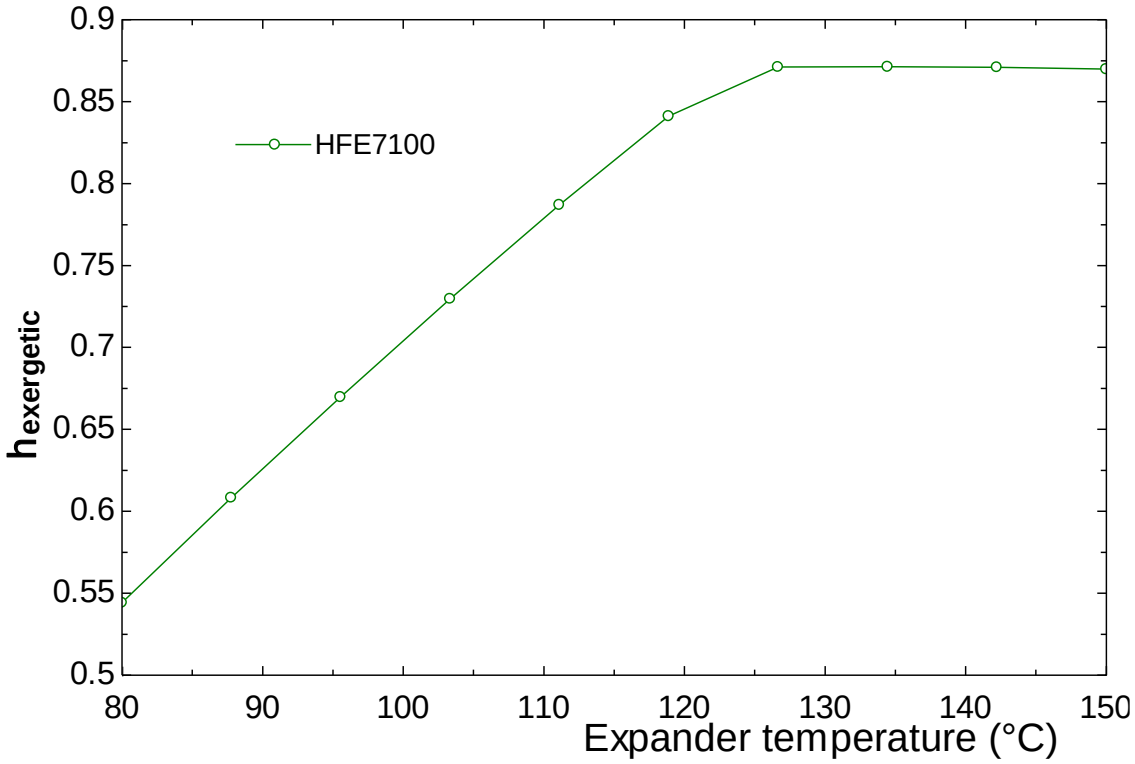

Figure 38: Exergetic Efficiency of regeneration Cycle With HFE7100

Above figure show the incremental increase of exergetic efficiency of regeneration cycle with increase in expander inlet temperature. Here efficiency of pump and of turbine are taken as 0.60 and 0.80 respectively. There is gradual increase in efficiency of cycle for fluid HFE7100. The variation of temperature is from 80-150 C and the change in the exergetic efficiency is from 0.55 to 0.8 till 120˚C and after that gradual increase then from 130-150˚C gradually the same efficiency of 0.85.

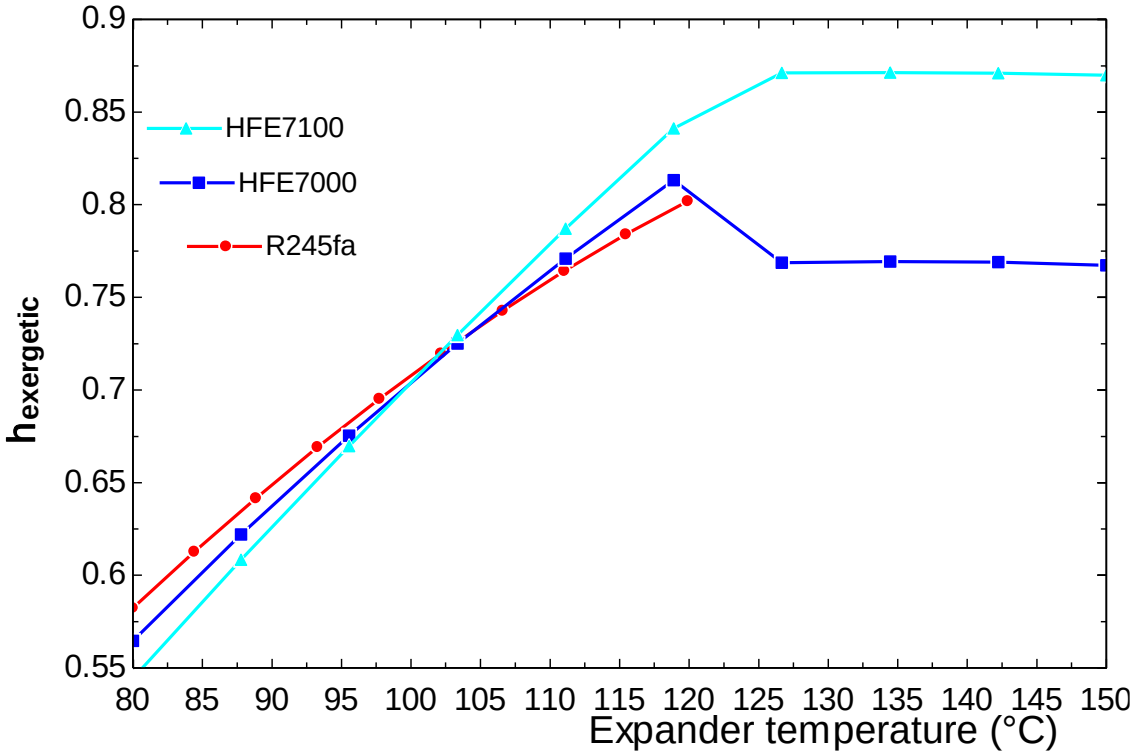

Figure 39: comparison of Exergetic Efficiency of regeneration Cycle With R245fa, HFE7000 and HFE7100

Above figure shows comparison in the exergetic efficiency of regeneration cycle with increase in expander inlet temperature. Here efficiency of the pump and turbine are taken as 0.60 and 0.80 respectively. There is gradual increase in efficiency of cycle for the fluid R245fa , HFE7000 and HFE7100. The variation of temperature is from 80-150˚C and the change in the exergetic efficiency is from 0.55 to 0.8 till 120˚C and after that gradual increase then from 130-150˚C gradually the same efficiency of 0.85. Maximum exergetic efficiency is for HFE7100.

4.2.3 Organic Rankine Cycle with Heat Exchanger

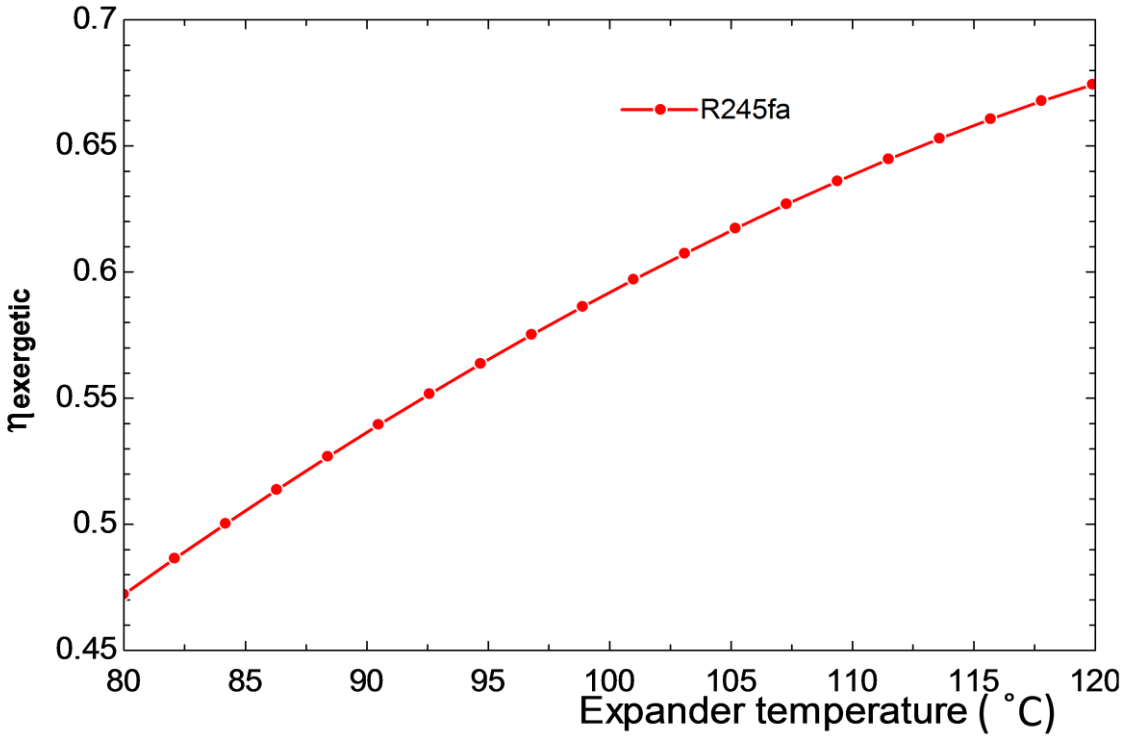

Figure 40: Exergetic efficiency of organic Rankine Cycle with heat exchanger with R245fa

Above figure shows the increase in exergetic efficiency of organic Rankine cycle with heat exchanger increase in expander inlet temperature. Here efficiency of pump and turbine are taken as 0.60 and 0.80 respectively. There is gradual increase in efficiency of cycle for fluid R245fa. The variation of temperature is from 80-120˚C and the change in the exergetic efficiency is from 0.4 to 0.67.

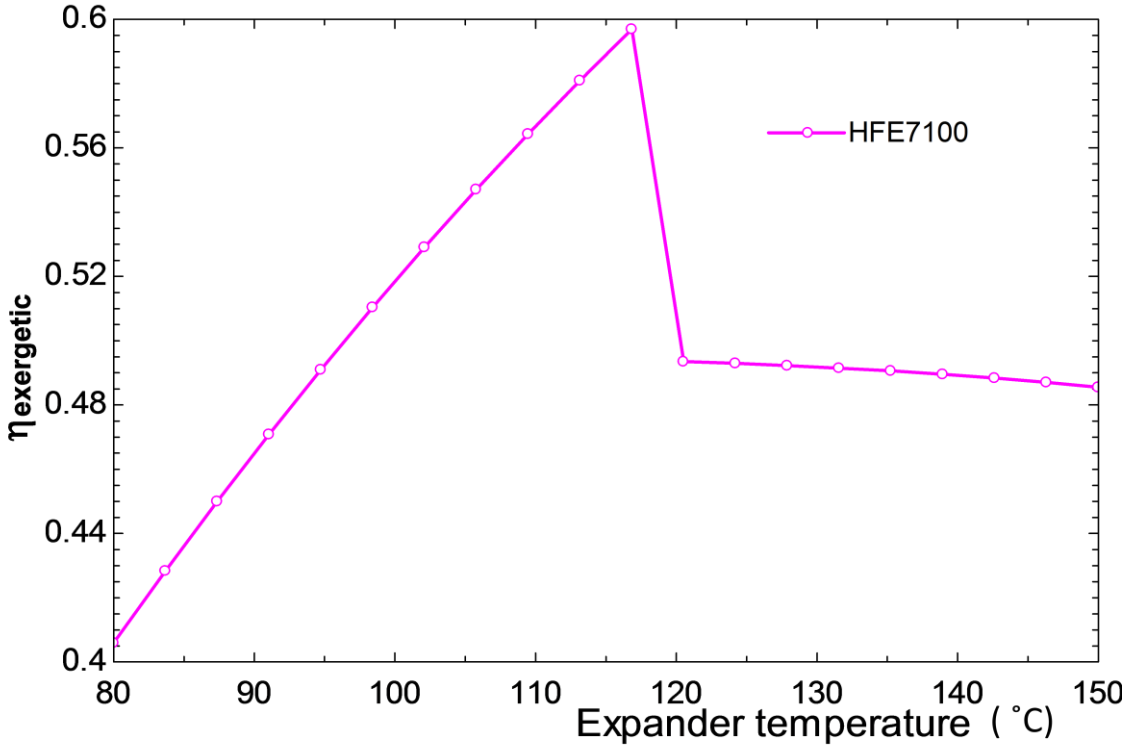

Figure 41: Exergetic Efficiency of organic Rankine Cycle With heat exchanger with HFE7100

Above figure show the increase in exergetic efficiency of organic Rankine cycle with heat exchanger, increase in expander inlet temperature. Here efficiency of the pump and of turbine are taken as 0.60 and 0.80 respectively. There is gradual increase in efficiency of cycle for the fluid HFE7100. The variation of temperature is from 80-150˚C and the change in the exergetic efficiency is from 0.4 to 0.6 After that the gradual decrease then from 120-150˚ C , the efficiency become merely constant i.e. 0.50.

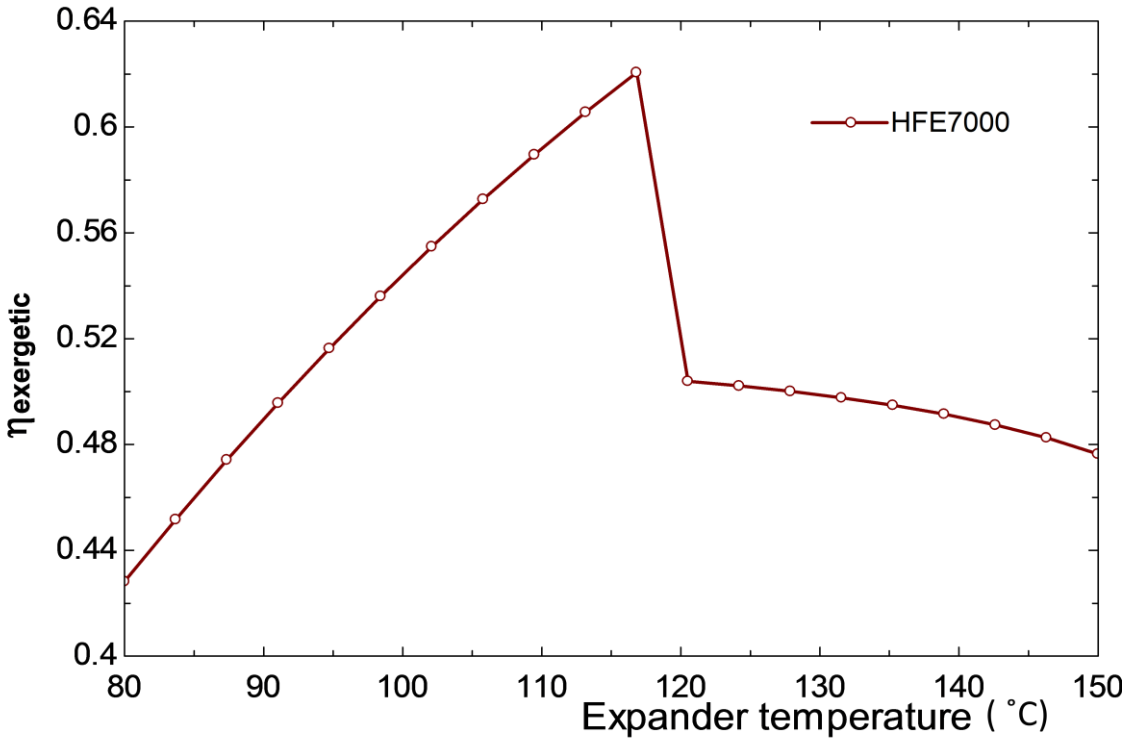

Figure 42: Exergetic Efficiency of organic Rankine Cycle With heat exchanger with HFE7000

Above figure show the increase in exergetic efficiency of organic Rankine cycle with heat exchanger, increase in the expander inlet temperature. Here efficiency of pump and turbine are taken as 0.60 and 0.80 respectively. There is gradual increase in efficiency of cycle for fluid HFE7000. The variation of temperature is from 80-150˚C and the change in the exergetic efficiency is from 0.42 to 0.65. After that the gradual decrease then from 120-150˚C , the efficiency become merely constant i.e. 0.50.-0.48.

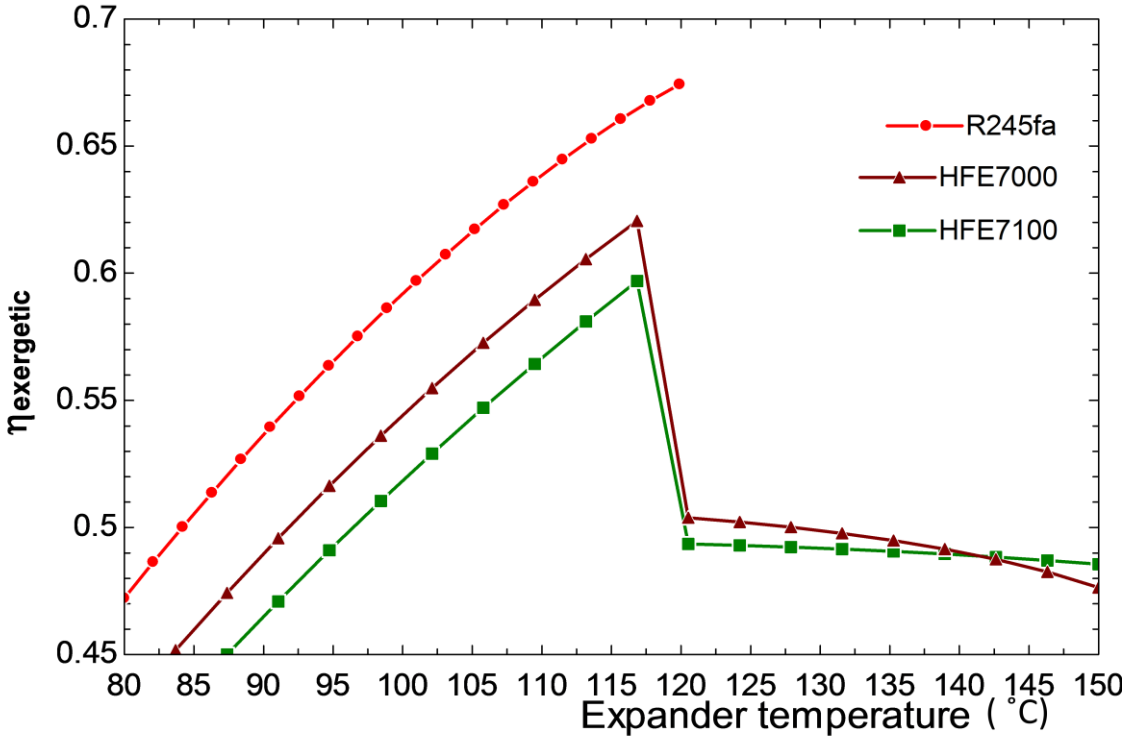

Figure 43: comparison of Exergetic Efficiency of organic Rankine Cycle With heat exchanger with R245fa, HFE7000 and HFE7100

Above figure show the comparison of increase in the exergetic efficiency of organic Rankine cycle with heat exchanger, with increase in expander inlet temperature. Here efficiency of pump and of turbine are taken as 0.60 and 0.80 respectively. There is gradual increase in efficiency of the cycle for the fluid R245fa , HFE7000 and HFE7100. The variation of temperature is from 80-150˚C and the change in the exergetic efficiency is from 0.55 to 0.8 till 120˚C and after that gradual increase then from 130-150˚C gradually the same efficiency of 0.85. Maximum exergetic efficiency is for R245fa i.e. 0.67.

CHAPTER 5

CONCLUSIONS AND FUTURE SCOPES

5.1 Conclusions

From the results presented in chapter 4 it can be concluded that:

For the saturated cycle with HFE7000 , R245fa and HFE7100 for the first order thermodynamic efficiency, there is gradual increase in the efficiency of the cycle for the fluid R245fa. The variation of temperature is from 80-130˚C and the change in the efficiency is from 9% to 12%. Maximum efficiency is for R245fa. on the other hand, for the ORC with heat exchanger and feed water heater, there is gradual increase in the efficiency of the cycle for the fluid R245fa. The variation of temperature is from 80-150˚C and the change in the efficiency is from 12%-17%. Maximum efficiency is for R245fa as comparison with HFE7000 and HFE 7100 the best suited result can be computed from HFE7000. On a fixed operating fluid rate, the thermal efficiency of the established ORC system could be enhanced with an increased heat source temperature. On the other hand, at a steady heat source temperature, the effective fluid pump rate can be optimised to get best-suited system thermal efficiency. The source temperature and ORC pump rate were significant parameters while plotting system thermal efficiency and the segment operations.

From exergetic analysis it can be concluded that:

For ORC with heat exchanger the variation of temperature is from 80-150˚C and the change in the exergetic efficiency is from 0.55 to 0.8 till 120˚C and after that gradual increase then from 130-150˚C gradually the same efficiency of 0.85. Maximum exergetic efficiency is for R245fa i.e. 0.67.

from the comparison of increase in exergetic efficiency of regeneration cycle with increase in expander inlet temperature. Here efficiency of pump and of turbine are taken as 0.60 and 0.80 respectively. There is gradual increase in the efficiency of cycle for the fluid R245fa , HFE7000 and HFE7100. The variation of temperature is from 80-150˚C and the change in the exergetic efficiency is from 0.55 to 0.8 till 120˚C and after that gradual increase then from 130-150˚C gradually the same efficiency of 0.85. Maximum exergetic efficiency is for HFE7100.

5.2 Future Scope

More of the work cane done on different fluids of merely same range of critical point temperature. Also different cycle can be incorporated for this, so as to get the better result.

Also prominent study can be done to get the best suited result for the heat exchanger and feed water pump so as to get increasingly exergetic efficiency and first order efficiency.

REFERENCES

1. Engineering Thermodynamics fifth edition P K Nag

2. https://powermin.nic.in/en/content/power-sector-glance-all-india (accessed on 20 may 2018).

3.Soteris A. Kalogirou, "Solar thermal collectors and applications", Progress in Energy and Combustion Science, Volume 30, Issue 3,2004,Pages 231-295,ISSN 0360-1285.

4.types of solar collectors, http://prashantkarhade.com/introduction-to-solar-thermal-technology/ (accessed on 20 may 2018).

5.Parabolic trough technology principle (left), https://www.volker-quaschning.de/articles/fundamentals2/index.php

6.SEGS parabolic trough plant in California (right) [NREL], http://www.newenergyupdate.com/csp-today/technology/parabolic-trough-technology-technical-advances-speed-csp-toward-grid-parity.

7.Layout of a linear Fresnel collector https://www.builditsolar.com/Projects/Concentrating/SOLRCONC_files/

8.Kimberlina linear Fresnel power plant, http://analysis.newenergyupdate.com/csp-today/markets/indias-pv-led-solar-growth-casts-eyes-performance-csp-projects

9.Dish Stirling system principle , http://cleanleap.com/7-solar-technology-assessment-and-appropriate-technology-options/71-solar-thermal-technology

10. Liu, H., Shao, Y., & Li, J. (2011). A biomass-fired micro-scale CHP system with organic Rankine cycle (ORC)–Thermodynamic modelling studies. Biomass and Bioenergy, 35(9), 3985-3994.

11.Wang, X. D., Zhao, L., Wang, J. L., Zhang, W. Z., Zhao, X. Z., & Wu, W. (2010). Performance evaluation of a low-temperature solar Rankine cycle system utilizing R245fa. Solar energy, 84(3), 353-364.

12. Borsukiewicz-Gozdur, A. (2013). Pumping work in the organic Rankine cycle. Applied Thermal Engineering, 51(1-2), 781-786.

13. Helvaci, H. U., & Khan, Z. A. (2015). Mathematical modelling and simulation of multiphase flow in a flat plate solar energy collector. Energy Conversion and Management, 106, 139-150.

14. Wang, H., Li, H., Wang, L., & Bu, X. (2017). Thermodynamic analysis of organic rankine cycle with hydrofluoroethers as working fluids. Energy Procedia, 105, 1889-1894.

15. Guo, S., Liu, D., Chen, X., Chu, Y., Xu, C., Liu, Q., & Zhou, L. (2017). Model and control scheme for recirculation mode direct steam generation parabolic trough solar power plants. Applied Energy, 202, 700-714.

16. Lobón, D. H., Baglietto, E., Valenzuela, L., & Zarza, E. (2014). Modeling direct steam generation in solar collectors with multiphase CFD. Applied Energy, 113, 1338-1348.

17. Quoilin, S., Van Den Broek, M., Declaye, S., Dewallef, P., & Lemort, V. (2013). Techno-economic survey of Organic Rankine Cycle (ORC) systems. Renewable and Sustainable Energy Reviews, 22, 168-186.

18. Wang, J., Yan, Z., Zhao, P., & Dai, Y. (2014). Off-design performance analysis of a solar-powered organic Rankine cycle. Energy Conversion and Management, 80, 150-157.

19. Ravelli, S., Franchini, G., Perdichizzi, A., Rinaldi, S., & Valcarenghi, V. E. (2016). Modeling of Direct Steam Generation in Concentrating Solar Power Plants. Energy Procedia, 101, 464-471.

20. Żywica, G., Kaczmarczyk, T. Z., Ihnatowicz, E., & Turzyński, T. (2017). Experimental investigation of the domestic CHP ORC system in transient operating conditions. Energy Procedia, 129, 637-643.

21. Odeh, S. D., Morrison, G. L., & Behnia, M. (1998). Modelling of parabolic trough direct steam generation solar collectors. Solar energy, 62(6), 395-406.

22. Guo, S., Liu, D., Chu, Y., Chen, X., Shen, B., Xu, C., ... & Wang, P. (2016). Real-time dynamic analysis for complete loop of direct steam generation solar trough collector. Energy Conversion and Management, 126, 573-580.

23. Biencinto, M., Montes, M. J., Valenzuela, L., & González, L. (2017). Simulation and comparison between fixed and sliding-pressure strategies in parabolic-trough solar power plants with direct steam generation. Applied Thermal Engineering, 125, 735-745.

24. Guo, J., Huai, X., & Cheng, K. (2018). The comparative analysis on thermal storage systems for solar power with direct steam generation. Renewable Energy, 115, 217-225.

25. Li, L., Sun, J., & Li, Y. (2017). Thermal load and bending analysis of heat collection element of direct-steam-generation parabolic-trough solar power plant. Applied Thermal Engineering, 127, 1530-1542.

26. Seitz, M., Cetin, P., & Eck, M. (2014). Thermal storage concept for solar thermal power plants with direct steam generation. Energy Procedia, 49, 993-1002.

27. Serrano-Aguilera, J. J., Valenzuela, L., & Parras, L. (2014). Thermal 3D model for direct solar steam generation under superheated conditions. Applied Energy, 132, 370-382.

28. Cheng, Z. D., He, Y. L., Xiao, J., Tao, Y. B., & Xu, R. J. (2010). Three-dimensional numerical study of heat transfer characteristics in the receiver tube of parabolic trough solar collector. International Communications in Heat and Mass Transfer, 37(7), 782-787.

29. Kuravi, S., Trahan, J., Goswami, D. Y., Rahman, M. M., & Stefanakos, E. K. (2013). Thermal energy storage technologies and systems for concentrating solar power plants. Progress in Energy and Combustion Science, 39(4), 285-319.

30. Dheep, G. R., & Sreekumar, A. (2015). Influence of accelerated thermal charging and discharging cycles on thermo-physical properties of organic phase change materials for solar thermal energy storage applications. Energy conversion and management, 105, 13-19.

31. Chacartegui, R., Vigna, L., Becerra, J. A., & Verda, V. (2016). Analysis of two heat storage integrations for an Organic Rankine Cycle Parabolic trough solar power plant. Energy Conversion and Management, 125, 353-367.

32. Bellan, S., Gonzalez-Aguilar, J., Romero, M., Rahman, M. M., Goswami, D. Y., Stefanakos, E. K., & Couling, D. (2014). Numerical analysis of charging and discharging performance of a thermal energy storage system with encapsulated phase change material. Applied thermal engineering, 71(1), 481-500

APPENDIX-1

1. Program For Saturated Cycle:

t3=80

x3=1

t1=30

t1=t4

eta_t=0.80

eta_p=0.6

x1=0

To=298.15

Th=373.15

h3=Enthalpy(R245fa,T=T3,x=x3)

s3=Entropy(R245fa,T=T3,x=x3)

s4s=s3

h4s=Enthalpy(R245fa,s=s4s,P=P4)

P4=P_sat(R245fa,T=T4)

eta_t=(h3-h4)/(h3-h4s)

s4=Entropy(R245fa,h=h4,P=P4)

s1=s2s

eta_p=(h2s-h1)/(h2-h1)

wt_s=(h3-h4s)

wt_a=(h3-h4)

h1=Enthalpy(R245fa,T=T1,x=x1)

s1=Entropy(R245fa,T=T1,x=x1)

s2=Entropy(R245fa,h=h2,P=P2)

P_sat3=P_sat(R245fa,T=T3)

wp_s=v1*(p_sat3-p_sat4)

h2s=h1+wp_s

P_sat3=P2

P_sat4=P_sat(R245fa,T=T4)

v1=Volume(R245fa,T=T1,x=x1)

PC3=P_crit(R245fa)

wp_a=h2-h1

qs=h3-h2

eta_cycle=(wt_a-wp_a)/qs

I_t=To*(s4-s3)

I_t1=(h3-To*s3-h4+To*s4)-wt_a

I_c=h4-To*s4-h1+To*s1

I_ev=To*((s3-s2)-(h3-h2)/th)

I_p=To*(s2-s1)

I_tot=I_t+I_p+I_c+I_ev

eta_ex=(EF-I_tot)/EF

EF=E_in

E_in=qs*(1-To/th)+wp_a

eta_ex1=wt_a/E_in

2. Program For ORC With Feed Water Heater:

```
t1=20

P1=P_sat(R245fa,T=T1)

x1=0

h1=Enthalpy(R245fa,T=T1,x=x1)

s1=Entropy(R245fa,T=T1,x=x1)

s1=s2

t8=80

P8=P_sat(R245fa,T=T8)

p5=p8

p4=p8

t5=120

h5=Enthalpy(R245fa,T=T5,P=P5)

s5=Entropy(R245fa,T=T5,P=P5)

p6=334

p6=p2

h2=Enthalpy(R245fa,s=s2,P=P6)

x3=0

h3=Enthalpy(R245fa,x=x3,p=p6)

s3=Entropy(R245fa,x=x3,P=P6)

s3=s4

h4=Enthalpy(R245fa,s=s4,P=P4)
```

p1=p7

h7=Enthalpy(R245fa,s=s7,P=P7)

s5=s6

s6=s7

h6=Enthalpy(R245fa,s=s6,P=P6)

wt_without=h5-h7

(1-m)*h2+(m)*h6=h3

wt_fd=1*(h5-h6)+(1-m)*(h6-h7)

wp_without=h2-h1

wp_fd=(1-m)*(h2-h1)+1*(h4-h3)

qs_fd=h5-h4

eff_cyclefd=(wt_fd-wp_fd)/qs_fd

I_t=to*(s7-s5)+m*(s6-s7)

to=20+273

I_p=to*((1-m)*(s2-s1)+(s4-s3))

I_evp=to*((s5-s4)-(h5-h4)/th)

th=130+273

{I_con=(1-m)*to*((s1-s7)+(h7-h1)/to)}

I_con=(1-m)*(h7-to*s7-(h1-to*s1))

I_fd=(s3-s2)+m*(s2-s6)

I_tot=I_p+I_evp+I_t+I_con+I_fd

Ex_in=qs_fd*(1-to/th)+wp_fd

eta_ex=1-(I_tot/Ex_in)

eta_ex1=wt_fd/Ex_in

3. Program For ORC With Heat Exchanger

```
eta_p=0.60

eta_t=0.80

t4=80

P4=P_sat(HFE7100,T=T4)

x4=1

h4=Enthalpy(HFE7100,x=x4,P=P4)

s4=Entropy(HFE7100,T=T4,x=1)

t5=120

h5=Enthalpy(HFE7100,T=T5,P=P4)

s5=Entropy(HFE7100,T=T5,P=P4)

t1=30

x1=0

P1=P_sat(HFE7100,T=T1)

h1=Enthalpy(HFE7100,T=T1,x=x1)

s1=Entropy(HFE7100,T=T1,x=x1)

s1=s2s

h2s=Enthalpy(HFE7100,s=s2s,P=P4)

eta_p=(h2s-h1)/(h2-h1)

s5=s6s

h6s=Enthalpy(HFE7100,s=s6s,P=P1)

eta_t=(h5-h6)/(h5-h6s)
```

s6=Entropy(HFE7100,h=h6,P=P1)

s2a=Entropy(HFE7100,h=h2a,P=P4)

eff=0.25

h6a=h6-h2a+h2

eff=(h6-h6a)/(h6-h2)

s6a=entropy(HFE7100,h=h6a,p=p1)

wt_s=h5-h6s

v1=volume(HFE7100,T=T1,x=x1)

wp_s=v1*(p4-p1)

wp_a=wp_s/eta_p

T2=Temperature(HFE7100,P=p4,h=h2)

T2a=Temperature(HFE7100,P=P4,h=h2a)

T6=Temperature(HFE7100,P=P1,h=h6)

T6a=Temperature(HFE7100,P=P1,h=h6a)

x3=0

h3=Enthalpy(HFE7100,x=x3,P=P4)

s2=Entropy(HFE7100,h=h2,P=P4)

h7=Enthalpy(HFE7100,x=1,P=P1)

s7=Entropy(HFE7100,x=x1,P=P1)

wt=h5-h6

w_net=wt-wp_a

qs=h5-h2a

qc=h6a-h1

eta_cycle=w_net/qs

to=298

I_t=to*(s6-s5)

I_p=to*(s2-s1)

I_evp=to*((s5-s2a)-(h5-h2a)/th)

th=130+273

I_c=to*((s1-s6a)-(h1-h6a)/to)

I_IHE=to*((s2a-s2)+(s6a-s6))

I_tot=I_c+I_evp+I_t+I_p+I_IHE

Ex_in=qs*(1-to/th)+wp_a

eta_ex=(Ex_in-I_tot)/Ex_in

eta_ex1=wt/Ex_in: